

Universitätsklinikum Hamburg-Eppendorf

Institut für Neuropathologie

Prof. Dr. med. Markus Glatzel

**Using small chemical compounds to inhibit polymerization
of neuroserpin in FENIB**

Dissertation

zur Erlangung des Grades eines Doktors der Medizin an der Medizinischen
Fakultät der Universität Hamburg.

vorgelegt von:

Thies Frieder Ingwersen
aus Leimen

Hamburg 2020

(wird von der Medizinischen Fakultät ausgefüllt)

**Angenommen von der
Medizinischen Fakultät der Universität Hamburg am: 11.01.2021**

**Veröffentlicht mit Genehmigung der
Medizinischen Fakultät der Universität Hamburg.**

Prüfungsausschuss, der/die Vorsitzende: Prof. Dr. Friederike Cuello

Prüfungsausschuss, zweite/r Gutachter/in: Prof. Dr. Markus Glatzel

Prüfungsausschuss, dritte/r Gutachter/in:

Contents

1	Introduction	5
1.1	Familial Encephalopathy with Neuroserpin Inclusion Bodies (FENIB)	5
1.1.1	Collins bodies as the neuropathological hallmark of FENIB	5
1.1.2	Pathophysiology of serpinopathies	7
1.1.3	Neuroserpin mutants cause conformational instability . . .	9
1.1.4	Conformational instability determines severity of FENIB .	11
1.1.5	Are symptoms found in FENIB the result of a gain or loss of neuroserpin function?	13
1.2	Neuroserpin — an inhibitor of tissue-type plasminogen activator .	14
1.3	Neuroserpin’s role in disease	15
1.3.1	Epilepsy	15
1.3.2	Stroke	16
1.3.3	Alzheimer’s disease	17
1.3.4	Schizophrenia	17
1.4	Possible treatment approaches in FENIB and other serpinopathies	18
1.4.1	Gene therapy	18
1.4.2	Reduce production of misfolded protein using RNAi	19
1.4.3	Increase clearance of polymers	19
1.4.4	Using small chemical compounds to prevent polymerization	20
2	Methods and Materials	22
2.1	Compounds	22
2.2	<i>In vitro</i> screening assay with recombinant neuroserpin	24
2.3	Cell culture	24
2.3.1	Compound concentrations	25
2.3.2	Screening experiment	26
2.3.3	Immunocytochemistry	26
2.4	Polyacrylamide gel electrophoresis	27
2.5	Western Blotting	29
2.6	Statistical analysis	30

3	Results	32
3.1	<i>In vitro</i> screening assay with recombinant neuroserpin	32
3.2	<i>In vivo</i> screening assay with a FENIB cell model	46
3.2.1	Characterization of the FENIB cell model	46
3.2.2	Determination of suitable concentrations of compounds for treatment	46
3.2.3	Screening compounds in a HEK-cell-model of FENIB	47
4	Discussion	56
4.1	Compound BUR reduces polymerization of recombinant wild type neuroserpin (NS ^{WT})	57
4.2	Recombinant NS ^{G392E} consists primarily of polymers prior to in- cubation	58
4.3	NS ^{G392E} cells are a suitable cell culture model of FENIB	59
4.4	Compound G enhances polymer retention <i>in vivo</i>	60
4.5	Conclusions	62
	Abstract	63
	Bibliography	65
	Acknowledgements	77
	Curriculum Vitae	78
	Eidesstattliche Versicherung	79

1 Introduction

1.1 Familial Encephalopathy with Neuroserpin Inclusion Bodies (FENIB)

1.1.1 Collins bodies as the neuropathological hallmark of FENIB

In 1986, Yerby et al. described an unusual case of Progressive Myoclonic Epilepsy (PME) and dementia in a 33-year-old woman from Portland, Oregon.

A brain biopsy of the frontal gyrus revealed numerous eosinophilic inclusions in the deeper layers of the cortex. The round-to-oval inclusions were mostly homogeneous and 10 μm to 50 μm in diameter. Moreover, they were strongly periodic acid–Schiff (PAS)-positive and diastase-resistant (Figure 1.1, A and B)(Yerby et al., 1986).

When examined by electron microscopy, the inclusions appeared to be composed of a fine granular homogeneous material free of filaments or fibrils (Yerby et al., 1986). Also, the inclusions seem to be confined to neurons and therein be enclosed by rough endoplasmic reticulum (ER) (Figure 1.1, C and D)(Davis et al., 1999a).

A number of similar PME cases with comparable neuropathological findings have been described before. However, regarding the etiology, only assumptions were voiced and these case reports remained undiagnosed (Bergener and Gerhard, 1970, Berkovic et al., 1986a,b, Dastur et al., 1966, Dolman, 1975, Ota et al., 1974).

By their histological appearance, the inclusions resembled the depositions found in Lafora disease, a rare genetic disorder that is also characterized by severe neurodegeneration leading to PME and cognitive decline (Yerby et al., 1986).

In Lafora disease, loss-of-function mutations in one of two genes (laforin or malin) involved in the glycogen metabolism cause deposits of abnormal glycogen accumulating into Lafora bodies within the cytoplasm of various tissues (Nitschke et al., 2018).

However, several clues pointed towards a different cause for the symptoms found in the 33-year-old woman from Portland: Lafora disease usually starts at the beginning of the second decade of life and patients rarely live past the age of twenty-five. Moreover, the so called Lafora bodies are not confined to the brain but can also be found in heart, liver, muscle, and skin tissue (Nitschke et al., 2018).

A muscle biopsy from the female patient showed no abnormalities (Yerby et al., 1986). Moreover, when examined by electron microscopy, cytoplasmic Lafora bodies present as glycogen like granules scattered with fine filaments; in contrast to the homogeneous inclusions confined by rough ER found in the described patient (Davis et al., 1999b, Nitschke et al., 2018).

The composition of the inclusion bodies found in the patient from Portland has not been identified for 13 years until similar inclusions were found in individuals of a large, unrelated family from Syracuse, New York. Affected family members encountered progressive cognitive decline leading to pre-senile dementia (Davis et al., 1999a,b). Autopsies revealed the same eosinophilic neuronal inclusions in the deeper layers of cerebral cortex and in many subcortical nuclei. White matter and cerebellar cortex showed only very few inclusions and non-neuronal tissues were free of them (Davis et al., 1999a).

Biochemical isolation and separation by sodium dodecyl sulfate (SDS)-polyacrylamide gel electrophoresis (PAGE) revealed them to be composed of a single 57 kDa protein. Further amino acid sequence analysis identified the protein as neuroserpin (NS), a serine protease inhibitor (serpin) of the brain. Moreover, immunohistochem-

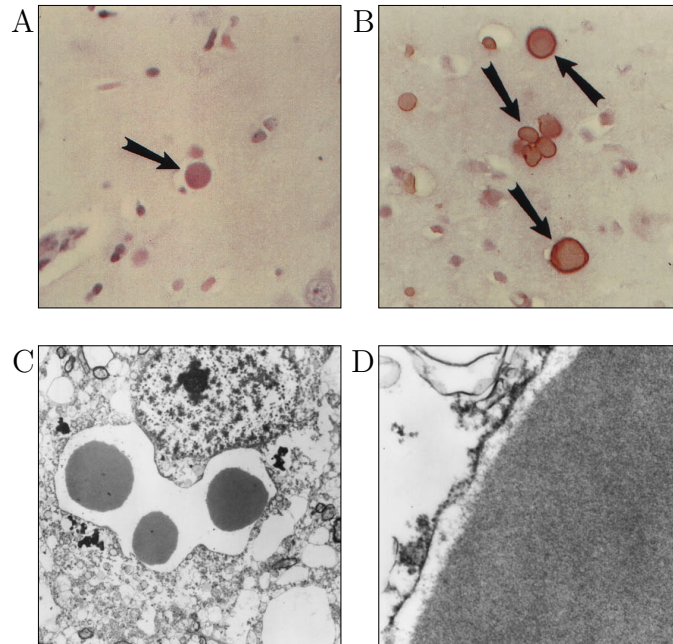


Figure 1.1: Representative depictions of Collins bodies. (A)-(B) show light microscopy at $400\times$ magnification stained with hematoxylin and eosin (H&E) and anti-NS-antibody, respectively. Arrows point at Collins bodies. (C)-(D) are electron microscopy images at $4000\times$ and $20000\times$ magnification, respectively. (Modified from Davis et al. (1999a))

ical analysis of the inclusions showed a positive staining with an anti-NS-antibody (Davis et al., 1999a,b).

Considering that these inclusions were distinctly different in appearance and composition to other known neuropathological entities, they were named Collins bodies after their first describer (Davis et al., 1999a,b).

Thus, it became apparent that the two families were affected by a novel neurodegenerative disease. Davis et al. (1999b) termed it Familial Encephalopathy with Neuroserpin Inclusion Bodies (FENIB).

1.1.2 Pathophysiology of serpinopathies

Familial Encephalopathy with Neuroserpin Inclusion Bodies (FENIB) joins the ranks of a group of diseases termed “conformational diseases” (Lomas and Carrell, 2002). The unifying characteristics of conformational diseases are the misfolding of proteins and a toxic overload of undegradable aggregations. Examples are A β -plaques in Alzheimer’s disease, misfolded prions in spongiform encephalopathies and polymerization of serine protease inhibitors (serpins) in serpinopathies.

Serpins are a large group of evolutionary conserved proteins with a wide range of physiological roles (Silverman et al., 2001). C1-inhibitor, α -1-antichymotrypsin, α -1-antitrypsin and NS are prominent members of the serpin superfamily.

The standard serpin fold consist of three beta sheets, nine alpha helices and a flexible reactive center loop (RCL) that acts as a pseudo-substrate for the target protease (Figure 1.2, A).

β -sheet A plays a key role in the main function of serpins — the inhibition of serine proteases. The inhibitory mechanism is initiated when the serpin’s flexible RCL comes in contact with the active site of the protease. A noncovalent intermediate Michaelis-complex is formed (Ye et al., 2001). After cleavage of the RCL by the protease, an ester bond is formed between the serpin’s RCL and the protease.

This triggers a conformational change within the serpin that results in the subsequent shift of the protease from one pole of the serpin to the other. The insertion of the cleaved RCL between strands 3A and 5A of β -sheet A traps the protease in this position (Wright and Scarsdale, 1995). The serpin-protease-complex can now be delivered to further proteolysis for permanent inactivation (Huntington et al., 2000).

In serpinopathies, specific mutants of these proteins are prone to form polymers that are retained within the ER (Roussel et al., 2011). The serpinopathy FENIB is caused by missense mutations in the NS gene resulting in polymerization of misfolded NS within the ER of neurons. Genetic testing of affected individuals of the families mentioned above show point mutations in the NS gene.

Mutations of residues near the so called shutter region in close proximity to β -sheet A can make a serpin prone to loop-sheet linkage (see Figure 1.2, A) (Silverman et al., 2001). The RCL of one serpin inserts between strands 3A and 5A of β -sheet A of another without interaction with a protease. The subsequent continuation of this loop-sheet linkage results in the formation of polymers and loss of function of the serpin (Figure 1.3) (Silverman et al., 2001).

The pathophysiology of FENIB has been investigated in several cell culture (Kroeger et al., 2009, Ying et al., 2011) and mouse models (Schipanski et al., 2013, 2014). These studies confirm ER retention of NS polymers previously described for FENIB patients using electron microscopy (Davis et al., 1999b). Furthermore, they suggest that polymers are targeted by endoplasmic-reticulum-associated protein degradation (ERAD), a cellular pathway that transports misfolded proteins from the ER to the ubiquitin proteasome system (UPS) for degradation (Kroeger et al., 2009, Schipanski et al., 2013, 2014, Ying et al., 2011).

Therefore, it has been suggested that exhaustion of ERAD and UPS may subsequently lead to the increasing accumulation of NS polymers — a process possibly

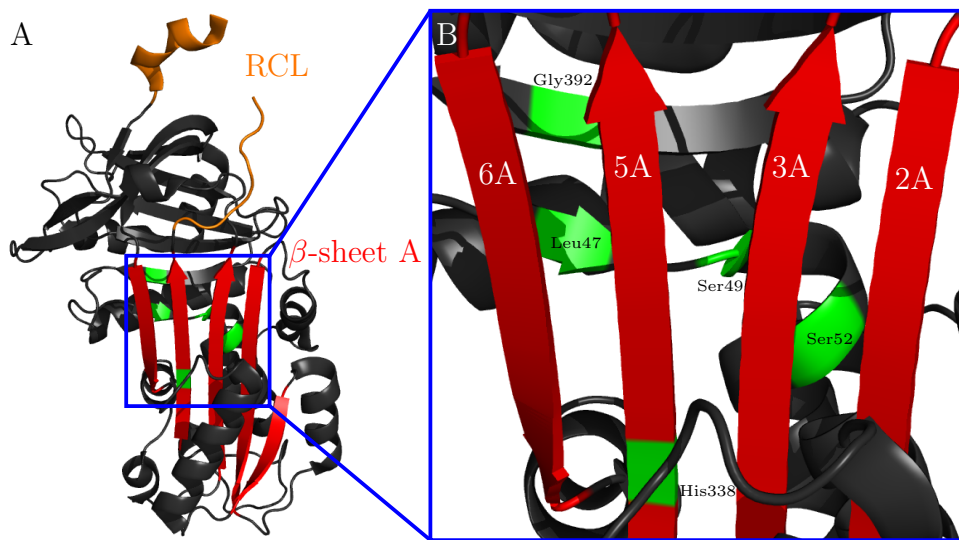


Figure 1.2: Molecular structure of NS and the shutter region. (A) shows the structural model of human NS. The RCL and β -sheet A are highlighted in orange and red, respectively. Part of the RCL was not detectable by crystallography due to its flexibility. The reported mutation sites (Leu47, Ser49, Ser52, His338, Gly392) are depicted in green. The blue square indicates the location of the shutter region. (B) shows the magnification of the shutter region with the same color coding. The five known mutation sites are in close proximity to strands 3A and 5A of β -sheet A. The figure was drawn using PyMOL and is based on the crystal structure of human NS (Protein Data Bank ID: 3FGQ).

accelerated by aging (Schipanski et al., 2013).

1.1.3 Neuroserpin mutants cause conformational instability

To date, six different single nucleotide substitutions in the NS gene have been identified that cause FENIB:

- T to C transition at nucleotide 140 (exon 2) resulting in an amino acid substitution of leucine 47 to proline (NS^{L47P}) (Hagen et al., 2011)
- T to C transition at nucleotide 226 (exon 2) resulting in an amino acid substitution of serine 49 to proline (NS^{S49P}) (Davis et al., 1999b)
- A to C transition at nucleotide 235 (exon 2) resulting in an amino acid substitution of serine 52 to arginine (NS^{S52R}) (Takao et al., 2000)
- A to G transition at nucleotide 1013 (exon 9) resulting in an amino acid substitution of histidine 338 to arginine (NS^{H338R}) (Davis et al., 2002)
- A to G transition at nucleotide 1174 (exon 9) resulting in an amino acid substitution of glycine 392 to arginine (NS^{G392R}) (Coutelier et al., 2008)
- G to A transition at nucleotide 1175 (exon 9) resulting in an amino acid substitution of glycine 392 to glutamate (NS^{G392E}) (Davis et al., 2002)

Figure 1.2 shows the molecular structure of NS and the localization of mutant residues within the shutter region nearby β -sheet A.

The closure of strands 3A and 5A is dependent on the correct expression of conserved aminoacids. Replacements at certain positions are thought to have a significant effect on the stability within β -sheet A.

Interestingly, the six known mutations in FENIB contribute in different amounts to the instability of NS (Figure 1.4)(Davis et al., 2002).

The substitution of serines 49 or 52 will destabilize the interaction of strands 3A and 5A. However, a charged and bulky arginine (as in NS^{S52R}) is predicted to cause greater perturbation within the shutter region than a smaller and uncharged proline would (as in NS^{S49P}) (Davis et al., 2002).

The replacement of leucine 47 by proline is thought to have a destabilizing effect similar in severity to the NS^{S52R} mutant (Hagen et al., 2011).

An even greater impact is expected for the substitution of histidine 338. Positioned in strand 5A, histidine's system of hydrogen bonds hold strand 3A and 5A together. A replacement of histidine with arginine results in the loss of these bonds and causes the opening of β -sheet A, making it vulnerable for loop insertion (Davis et al., 2002).

However, the most destructive instability is thought to be caused by the substitution of glycine 392 (Davis et al., 2002). The importance of this glycine is underlined by its consistent conservation within the serpin family. It is needed for the correct arrangement of adjacent phenylalanines and thereby crucial to the stability of the shutter region (Davis et al., 2002, Ryu et al., 1996).

Thus, a severity ranking from least to most destructive mutation can be expressed as follows (Davis et al., 2002):

$$\text{NS}^{\text{S49P}} < \text{NS}^{\text{S52R}}/\text{NS}^{\text{L47P}} < \text{NS}^{\text{H338R}} < \text{NS}^{\text{G392E}}/\text{NS}^{\text{G392R}}$$

Note that NS^{L47P} and NS^{G392R} were discovered more recently and, thus, were not discussed in the original study from Davis et al. (2002). Their conformational instability was estimated by the observed symptoms and neuropathological reports

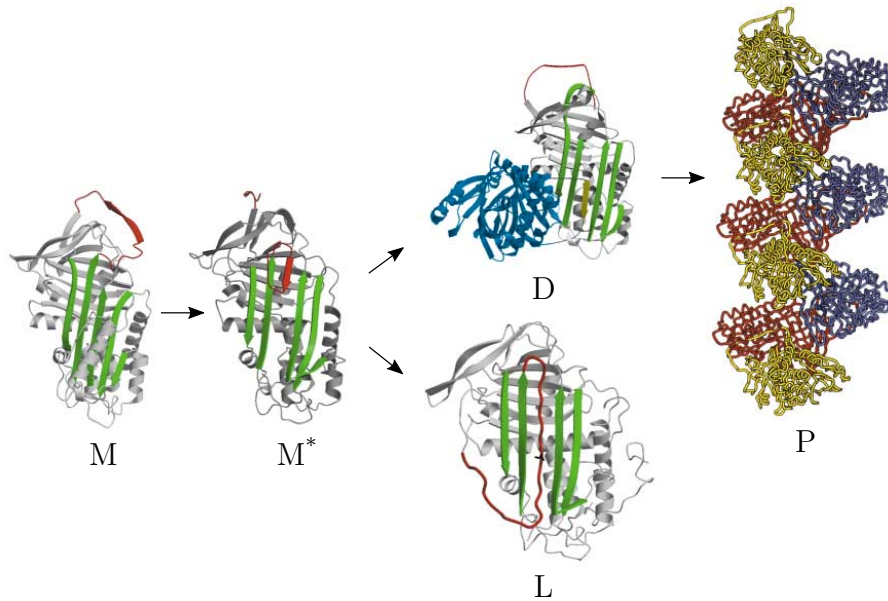


Figure 1.3: Polymerization mechanism of serpins. Certain mutations cause a conformational instability within the serpin molecule. The partial opening of β -sheet A (green) results in the insertion of the RCL (red) and the formation of an unstable intermediate (M^*). The RCL can then fully fold into β -sheet A, forming a latent serpin (L). Alternatively, β -sheet A accepts the RCL of a second serpin molecule (blue) forming a dimer (D) and subsequently polymers (P). Individual molecules in the polymer are colored in yellow, red and purple. (Modified from Lomas and Carrell (2002))

rather than structural considerations (Coutelier et al., 2008, Hagen et al., 2011).

1.1.4 Conformational instability determines severity of FENIB

These considerations correspond well with the observed neuropathology in affected patients. The number and size of Collins bodies increase with the predicted severity of mutations.

Patients carrying the mild NS^{S49P} allele show only few Collins bodies in the deeper layers of cortex — as is the case of the family from Syracuse (Davis et al., 1999a).

The PME patient from Portland and another unrelated family carrying the more severe NS^{S52R} mutation show approximately three times more inclusions (Davis et al., 1999a, Takao et al., 2000).

Patients positive for the most destructive NS^{H338R}, NS^{G392E} or NS^{G392R} alleles present with a considerable increase of inclusions. They can be found in most neurons and are sometimes clustered in groups of three or more (Coutelier et al., 2008, Davis et al., 2002, Ranza et al., 2017).

The acceleration of inclusion-body-formation could be demonstrated by histological examination. Those affected by a more severe mutant already had far more Collins bodies in autopsies or biopsies taken in the second or third decade of life than did patients with the mild NS^{S49P} allele after death in the sixth or seventh decade (Davis et al., 2002).

In addition, onset of disease seems to be a characterizing difference between mutants. The mildest form, NS^{S49P}, has the latest onset in the fifth or sixth decade of life. For the NS^{S52R} and NS^{L47P} allele an onset in the mid to late third decade of life seems to be typical. Carriers of the NS^{G392E} and NS^{H338R} allele seem to develop signs in the second decade of life (Davis et al., 2002, Ranza et al., 2017). In one patient with the NS^{G392R} allele first symptoms occurred as early as at the age of seven years (Ranza et al., 2017).

Not only does the degree of conformational instability correlate with the rate of inclusion-body-formation and the onset of disease, but also the range and severity of symptoms vary between mutants (Davis et al., 2002).

Patients carrying the NS^{S49P} allele develop cognitive decline accompanied by deterioration of attention and concentration (Davis et al., 1999a,b). As the disease progresses, most patients develop additional signs of frontal dysfunction, e.g. reduced oral fluency, perseveration, stereotypic behavior and motor-restlessness (Bradshaw et al., 2001). Also, impaired visuospatial skills become more apparent over time (Bradshaw et al., 2001, Davis et al., 1999b). Memory was also affected, but to a lesser extent than typically seen in Alzheimer's disease (Davis et al., 1999a,b). The relentless process of disease usually ends in institutional care and death after

approximately ten years (Bradshaw et al., 2001, Davis et al., 1999a,b, 2002).

The more disruptive mutations result in a more rapid progression of cognitive

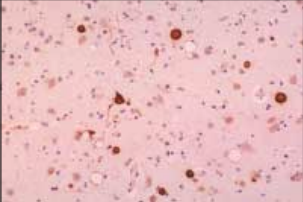
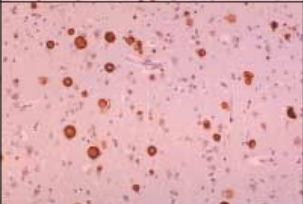
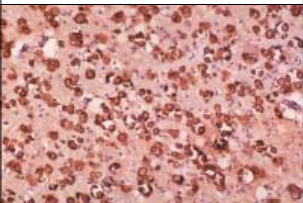
Mutation	Onset	Polymerization rate	Symptoms	Autopsy
NS ^{S49P}	48	+	Dementia, tremor, seizures in terminal stages	
NS ^{S52R}	24	++	Myoclonus, status epilepticus, dementia	
NS ^{L47P}	24	++	Myoclonus, tremor, dementia	N/A
NS ^{H338R}	15	+++	Myoclonic seizures, dementia, tremor, dysarthria	N/A
NS ^{G392E}	13	++++	Myoclonus, status epilepticus, dementia, chorea	
NS ^{G392R}	8	++++	Dementia, epilepticus of slow-wave sleep	N/A

Figure 1.4: Correlation of conformational instability, onset of symptoms and rate of polymerization. Mutations that cause a greater disruption to the conformation of NS have an earlier onset of symptoms (“onset” in years) and a higher rate of polymerization. Also, the severity of symptoms increases with growing instability. For those cases where an autopsy was performed a representative histological image at post-mortem is depicted. (Modified from Gooptu and Lomas (2009), Hagen et al. (2011))

decline (Davis et al., 1999b, Yerby et al., 1986).

However, the most noticeable difference of the more severe mutants (other than NS^{S49P}) is the occurrence of epilepsy. Several types of seizures have been reported in FENIB, including myoclonic, generalized tonic-clonic, absence and electrical status epilepticus in sleep (ESES). (Coutelier et al., 2008, Gourfinkel-An et al., 2007, Ranza et al., 2017).

Apart from cognitive deterioration, most clinical reports mention PME as the cardinal syndrome (Amano-Takeshige et al., 2018, Davis et al., 1999a, 2002, Gourfinkel-An et al., 2007, Hagen et al., 2011, Ranza et al., 2017, Takao et al., 2000, Yerby et al., 1986).

Furthermore, generalized tonic-clonic seizures, which are difficult to control with anti-epileptic drugs, often complicate the course of disease (Coutelier et al., 2008, Davis et al., 2002, Gourfinkel-An et al., 2007, Hagen et al., 2011, Takao et al., 2000). In fact, death by status epilepticus has been reported in a patient carrying the NS^{G392E} allele (Davis et al., 2002).

1.1.5 Are symptoms found in FENIB the result of a gain or loss of neuroserpin function?

The intriguing correlation of Collins-body-formation and onset and severity of symptoms suggests that the inclusions are neurotoxic (Davis et al., 1999b). Moreover, cell death and gliosis can often be linked to areas affected most by inclusions (Davis et al., 1999a, Hagen et al., 2011, Takao et al., 2000).

However, we know from other serpinopathies that not only accumulation of polymers (gain of function), but also the lack of inhibitory functions (loss of function) can contribute to disease (Belorgey et al., 2007).

The most prominent representative of serpinopathies is the α -1-antitrypsin deficiency (Roussel et al., 2011). It is one of the most common genetic diseases. In North Europe approximately 1:2000 are homozygotes for the severe Z allele (Glu342Lys) (Lomas et al., 2016).

α -1-antitrypsin is synthesized by the liver and released to the plasma at a concentration of 1.5 g L⁻¹ to 3.5 g L⁻¹. It is an inhibitor of neutrophil elastase, an enzyme secreted by neutrophils and macrophages during inflammation (Roussel et al., 2011).

Certain mutations result in polymerization and accumulation of α -1-antitrypsin mutants within the ER of hepatocytes. The protein overload is associated with liver cirrhosis and hepatocellular carcinoma. Loss of function leads to lung emphysema due to unregulated enzymatic stress by neutrophil elastase (Roussel et al., 2011).

Conversely, mutations that result in a mere loss of function but no accumulation of polymers cause emphysema only and no liver cirrhosis (e.g. Pi null mutation)

(Lomas et al., 2016).

Symptoms found in FENIB might not only be caused by the toxic effect of Collins bodies (gain of function), but also be the result of reduced amounts of functioning NS (loss of function).

It is noteworthy that the inhibitory effect of NS^{S49P} is not reduced *in vitro*. Only mutations causing a higher degree of instability lose their inhibitory function (Belorgey et al., 2002, 2004).

Therefore, both the residual activity of mutant NS and its polymerization rate may account for the symptom divergence between the six known mutations of FENIB.

The following chapter gives a brief overview of known physiological functions of NS.

1.2 Neuroserpin — an inhibitor of tissue-type plasminogen activator

NS was identified as an axonally secreted serpin mainly expressed by neurons of the central and peripheral nervous system. The NS gene was mapped on human chromosome 3 at position 3q26 and consists of nine exons. The first exon is non-coding, the remaining exons code for a 410 amino acids glycoprotein with an approximate mass of 55 kDa (Schrimpf et al., 1997).

Based on conserved residues within the RCL of serpins that act as pseudo-substrates for the target protease (Elliott et al., 1996, Ryu et al., 1996), it has been suggested that NS has an inhibitory function as well (Osterwalder et al., 1996). *In vitro* experiments have identified NS as a strong inhibitor of tissue-type plasminogen activator (tPA). A number of other serine proteases, including urokinase, trypsin and NGF- γ , are inhibited with a lower efficiency (Hastings et al., 1997, Osterwalder et al., 1998).

Furthermore, NS and tPA show widely shared expression patterns, suggesting that tPA is the main target (Krueger et al., 1997, Teesalu et al., 2004). This observation is further strengthened by a decrease in tPA activity measured in a transgenic mouse model overexpressing NS (Cinelli et al., 2001).

One of the first recognized functions of tPA is the regulation of thrombolysis in blood (Chevilley et al., 2015). tPA catalyses the conversion of plasminogen to plasmin, a protease that degrades fibrin and thus leads to the disintegration of blood clots. Due to the thrombolytic activity, recombinantly produced tPA (rtPA), such as alteplase, is routinely administered intravenously to attempt recanalisation in embolic or thrombotic strokes.

Within the brain, however, the pathways involving tPA are not yet as clearly defined. tPA is thought to play important roles in processes as diverse as neuronal

development and plasticity, axonal regeneration, microglial activation, excitotoxicity and blood–brain barrier (BBB) integrity (Fredriksson et al., 2015).

Whereas plasminogen activator inhibitor-1 (PAI-1) is thought to be the main inhibitor of tPA within the vascular system, studies have shown that NS is one of the principle inhibitor within the central nervous system (CNS) (Fredriksson et al., 2015). It is therefore thought to play an important role in these mechanisms by regulating the proteolytic activity of tPA.

Gene expression dynamics in mice during the late stages of neurogenesis suggest an important role for NS in neuronal migration, axonal outgrowth and synapse formation. During these stages of neuronal maturation, tPA is discussed to play an important role as well, further underlining the regulatory function of NS (Krueger et al., 1997).

Both NS and tPA have been discussed to be involved in neuronal plasticity (Reumann et al., 2017). Expression and secretion of both players are regulated by neuronal activity — a feature often observed to be important for molecules involved in neuronal plasticity (Lee et al., 2015, Miranda et al., 2008, Qian et al., 1993).

Additionally, neurite extension (Parmar et al., 2002), cell-cell-adhesion (Lee et al., 2008) and dendritic spike morphology (Borges et al., 2010) have shown to be dependent on NS expression level. NS-deficient mice present with significantly less spine-synapses within the hippocampal CA1-region.

1.3 Neuroserpin’s role in disease

NS has been studied in context of diseases other than FENIB. The following sections give a brief overview on neuroserpin’s role in these diseases.

1.3.1 Epilepsy

One of the striking differences between the NS^{S49P} variant and all other known mutants is the more frequent appearance of epileptic symptoms in the more severely disruptive mutants. While this may be explained by an increase in the number of inclusion bodies, a growing body of evidence suggests that part of it might result from a lack of the inhibitory function.

Early *in vitro* studies with recombinant NS^{S49P} and NS^{S52R} show that while enzymatic activity of NS^{S49P} is decreased, no inhibitory activity can be detected in NS^{S52R} (Belorgey et al., 2002, 2004).

NS seems to have a protective effect in mouse models of epilepsy. Treatment with NS dampens the neuronal excitability after injection with excitotoxic kainate (Yepes

et al., 2002). Moreover, NS deficient mice are more vulnerable to kainate than NS^{WT} mice (Fredriksson et al., 2015).

It has been hypothesised, that this is due to a tPA-dependent increase in BBB permeability. As an inhibitor of tPA, NS may play an important regulatory role in this (Fredriksson et al., 2015, Yepes et al., 2003). However, exact mechanisms are still under investigation. Recent research suggests that tPA influences the platelet-derived growth factor receptor α (PDGFR α) pathway (Fredriksson et al., 2015).

tPA is also involved in NMDR receptor related increase in excitability (Baron et al., 2010, Fernández-Monreal et al., 2004, Nicole et al., 2001, Samson et al., 2008). The administration of NS reduces lesion size after excitotoxic insult induced by NMDA injection into mouse brains. The excitotoxic effect of NMDA was dampened by the addition of NS in neuronal cell cultures, as well (Lebeurrier et al., 2005).

In conclusion, these studies suggest that epilepsy associated with FENIB is in part the result of a lack of the inhibitory effect of NS.

1.3.2 Stroke

In addition to the neuroprotective effect seen in models of epilepsy, NS has a positive outcome effect in animal models of ischemic stroke.

In rats that suffered from artificial middle cerebral artery (MCA) occlusions, the administration of NS reduced the infarct size (Yepes et al., 2000) and prolonged the therapeutic window of tPA (Zhang et al., 2002). This effect could not be achieved with cleaved NS that lost its inhibitory function suggesting an involvement of its primary target protease tPA (Yepes et al., 2000).

Transgenic mice overexpressing NS had smaller infarcts compared to wild type (Cinelli et al., 2001) in a MCA occlusion model. Moreover, the infarcts of NS knock-out mice were bigger (Gelderblom et al., 2013).

NS might reduce infarct volume by inhibition of tPA-mediated microglia activation (Gelderblom et al., 2013).

More evidence for a neuroprotective function comes from a mouse model investigating the effect of temporary acute retinal ischemia. Administering NS intravitreally prior to the ischemic attack reduces the number of apoptotic cells and weakens the loss of retinal function. Similar effects were demonstrated in tPA knock-out mice suggesting a tPA-independent function for NS (Gu et al., 2015).

Correlative studies in human stroke patients have shown that high concentrations of neuroserpin in blood samples are associated with better functional outcome (Rodríguez-González et al., 2011b) and reduced inflammation (Rodríguez-González et al., 2011a). However, attempts to find a relationship between neuroserpin polymorphisms in humans and likelihood of stroke have produced little evidence of pro-

tective neuroserpin variants (Cole et al., 2007, Tjärnlund-Wolf et al., 2011).

1.3.3 Alzheimer's disease

A key pathophysiological hallmark of Alzheimer's disease is the formation of amyloid- β -plaques ($A\beta$) in the brain. While the exact mechanisms of disease are still under extensive investigation, the hypothesis that $A\beta$ has a neurotoxic effect is widely accepted (Selkoe and Hardy, 2016).

NS was found to be associated with $A\beta$ -plaques in Alzheimer's disease (Fabbro and Seeds, 2009, Kinghorn et al., 2006) and is elevated in patients' cerebral fluid (Nielsen et al., 2007).

To date, the role NS plays in Alzheimer's is not conclusively explained. *In vitro* studies show that $A\beta_{1-42}$ and NS form a 1:1 binary complex. Moreover, NS increases the polymerization of $A\beta$ (Kinghorn et al., 2006).

In a cell culture, however, NS has a beneficial effect and reduces the cytotoxicity of $A\beta$.

Animal models have further elucidated this protective role of NS in Alzheimer's disease. Injected $A\beta$ is cleared slower in tPA-knockout mice and more rapidly in NS-knockout mice. This relationship may come from the activation of plasmin by tPA or the upstream inhibition by NS.

Further insights have resulted from knocking out NS in an Alzheimer's mouse model (transgenic J20 mice). These mice present with fewer and smaller $A\beta$ -plaques and a normal Morris water maze performance (Fabbro et al., 2011).

1.3.4 Schizophrenia

Gene expression was assessed using microarray analysis showing either an increase (Hakak et al., 2001) or decrease (Vawter et al., 2001) in NS expression levels in the dorsolateral prefrontal cortex in patients with schizophrenia. A real-time quantitative polymerase chain reaction (Q-PCR) study agrees with decreased NS levels (Vawter et al., 2004).

Although the data seems to be somewhat contradictory, altered NS levels in schizophrenia may be explained by its functions involving brain development (section 1.2) and neuroprotection (section 1.3). Since NS secretion is neuron activity dependent (Miranda et al., 2008, Parmar et al., 2002) it also seems conceivable that the changed expression level is due to uncontrolled activation as a consequence of the underlying disease (Lee et al., 2017).

1.4 Possible treatment approaches in FENIB and other serpinopathies

FENIB is a very severe neurological disease that leads to disabling cognitive decline and epilepsy. Attempts have been made to symptomatically treat reoccurring episodes of epilepsy with anticonvulsant drugs, including phenytoin, valproic acid, carbamazepine, piracetam, topiramate, levetiracetam, and ethosuximide, zonisamide, benzodiazepines and corticosteroids (Amano-Takeshige et al., 2018, Coute-lier et al., 2008, Hagen et al., 2011, Takao et al., 2000). However, the treatment often had very little or no effect. Furthermore, cognitive decline remains relentless. To date, no potent therapy has been developed to cure FENIB.

Thus, researcher seek to find a definite and causative treatment to effectively treat FENIB patients. The literature provides only little evidence for the prevention of NS polymerization. However, some attempts have been made. Moreover, there is a growing body of evidence for causal treatment of α -1-antitrypsin deficiency that could be applied for FENIB in future.

In this chapter, treatment concepts that are currently under investigation or discussion for serpinopathies are examined.

1.4.1 Gene therapy

Gene replacement therapy In some serpinopathies, the lack of correctly folded protein accounts for some or all of the symptoms. Examples of loss-of-function mutations are found in α -1-antitrypsin and α -1-antichymotrypsin (lung emphysema), antithrombin (thrombosis) or C1-inhibitor (angio-oedema) (Lomas et al., 2016). The lack of functioning protein can be tackled by either regular intravenous substitution (Lomas et al., 2016) or gene replacement therapy using adeno-associated viruses (AAV) (Saraiva et al., 2016). However, a phase II clinical trial with the attempt to introduce functioning α -1-antitrypsin to patients show only marginal results (Mueller and Flotte, 2013). Moreover, the misfolded protein still remains within the ER of hepatocytes, since the polymerizing variant is still expressed. Thus even a more potent gene replacement therapy would be ineligible for serpinopathies where symptoms rather arise from toxic polymers (gain-of-function).

Gene editing therapy In serpinopathies, a single point mutation causes the disease. This makes them vulnerable for techniques that can correct for such a single nucleotide substitution. First approaches have been tested for α -1-antitrypsin deficiency in induced pluripotent stem cells using zinc finger nucleases and a piggyBac donor vector (Yusa et al., 2011). Future gene therapies might include the CRISPR-

Cas9 method where precise genome editing is possible (Cong et al., 2013). This method has successfully been used to knock-out genes in mice brain (Platt et al., 2014). Correction of point mutations have also been reported (Komor et al., 2016).

However, safety and efficiency of gene therapy are still discussed.

1.4.2 Reduce production of misfolded protein using RNAi

Using RNA interference (RNAi)-based methods, specific mRNA can effectively be silenced by degradation (Fire et al., 1998). This method uses small interfering RNA (siRNA) that bind specifically to certain mRNA and eventually lead to the degradation by the RNA-induced silencing complex (RISC). This has already been established in experimental biology, but first approaches have been made to use this mechanism in treatment of genetic disorders.

Treatment with siRNA that have a liver motif has shown a reduction in production and aggregation of mutant α -1-antitrypsin in a mouse model of α -1-antitrypsin-deficiency. RNAi treatment also led to significant reduction in α -1-antitrypsin serum levels in non-human primates (Guo et al., 2014).

Currently a phase I/II trial is been conducted, to test safety of RNAi therapy in human with α -1-antitrypsin deficiency (identifier: NCT02503683). Considering the specificity and efficiency, siRNA could be developed as a possible treatment for other serpinopathies, including FENIB.

1.4.3 Increase clearance of polymers

Another approach to treat the aggregation of misfolded protein is to increase cellular clearance.

Carbamazepine, an anticonvulsant that has been clinically used for over half a century, has shown to also induce autophagy. A current clinical study is set out to investigate if the clearance of polymeric α -1-antitrypsin is also increased (identifier: NCT01379469). If inclusion body formation can be reduced in this study, carbamazepine would be a credible drug to test in FENIB as well, considering it's additional antiepileptic effect.

Another drug that has been in the focus of autophagy research is rapamycin. In an α -1-antitrypsin mouse model rapamycin showed an increase in autophagic clearance and a decrease in polymeric α -1-antitrypsin and liver damage (Kaushal et al., 2010).

1.4.4 Using small chemical compounds to prevent polymerization

In serpinopathies, the underlying mechanism of disease is the insertion of the RCL of one serpin into the β -sheet A of another. This concept has been exploited in attempts to inhibit polymerization by developing molecules that fit into the β -sheet A to block the RCL insertion.

Using small 6-mer and 4-mer peptides, a proof of principle could be shown for α -1-antitrypsin. The peptides, which were derived from RCL sequence, bound to α -1-antitrypsin and reduced polymerization *in vitro* (Chang et al., 2006, 2009, Mahadeva et al., 2002). However, the challenge to deliver these peptides inside the cells of affected organs remained unmet.

It has been argued that small molecules that bind to the β -sheet A are better suited to find their way inside the cells (Elliott et al., 2000, Mallya et al., 2007). Mallya et al. (2007) developed a virtual ligand screening method to identify small compounds that fit into a cavity in close proximity to β -sheet A of α -1-antitrypsin. Compounds were identified that blocked polymerization *in vitro* and in a cell model of disease.

Another strategy emerged with the identification of an antibody that prevents polymerization of α -1-antitrypsin *in vitro*. A single-chain variable fragment of this antibody could prevent up to 60 % of polymerization within the cells and significantly improve secretion when expressed as an intrabody in an α -1-antitrypsin cell model (Ordóñez et al., 2015). The epitope of this intrabody spans helices A and I. This is thought to stabilize β -sheet A and thus prevent RCL insertion (Motamedi-Shad et al., 2016).

The intrabody gene would have to be introduced to the cell using gene therapy methods. An advantage over RNAi would be that intrabodies are expressed more stable in mammalian cells than siRNA (Ordóñez et al., 2015).

To date, little research has been conducted regarding the inhibition of polymerization in FENIB. However, the data gathered for α -1-antitrypsin deficiency can be used as basis in the development of disease specific drugs for other serpinopathies including FENIB and vice versa. This is due to the structural and mechanistic similarities within serpins and serpinopathies.

Embelin is a compound that inserts into a cavity formed by helices D and F and strand 2A of β -sheet A of PAI-1. This antagonizes the inhibitory effect of PAI-1 (Lin et al., 2013).

Embelin has also shown to bind to NS and inhibit polymerization that occurs when recombinant NS is heated *in vitro* (Saga et al., 2016). No data regarding the effectivity *in vivo* is available.

The incentive of this study is to identify small chemical compounds that inhibit polymerization. Two large libraries of commercially available compounds were screened for molecules that mimic the RCL sequence G₃₄₈-S-E-A-A-A-V-S₃₅₅ of NS. For this, the crystal structure of cleaved human NS was used (Protein Data Bank ID: 3F02). Using the FlexX software, a virtual receptor docking screening assay was performed searching for ligands that bind to those amino acids that are in a 6.5 Å radius of the G₃₄₈-S-E-A-A-A-V-S₃₅₅ sequence. We hypothesize that these compounds inhibit polymerization by competing with the RCL over the insertion site of β -sheet A.

In this work, we tested 36 compounds for their anti-polymerogenic activity on NS^{G392E}, both *in vitro* using recombinant NS as well as in a FENIB cell culture model. Results from this work will be employed to further improve the *in silico* compound screening assay.

2 Methods and Materials

2.1 Compounds

Based on the crystal structure of cleaved human NS (Protein Data Bank ID: 3F02), an *in silico* model of reactive site loop insertion into β -sheet A was generated by molecular dynamics simulations. For this, the MolPort database of commercially available compounds (molport.com) was screened for ligands that mimic the G₃₄₈-S-E-A-A-A-V-S₃₅₅ sequence of the RCL. In a virtual receptor docking screening assay, the receptor was defined as those amino acids that are in a 6.5 Å radius of one of the atoms of this sequence. Compounds that bind to this virtual receptor were then identified.

This analysis was carried out by Johannes Kirchmair (Department of Chemistry and Computational Biology Unit, University of Bergen) using the FlexX software (BioSolveIT). The original *in silico* screening was later refined to improve the mimicking of the RCL sequence. Compounds of the first and second screening are hereafter referred to as 1st and 2nd generation compounds, respectively.

The chemical compounds were delivered in powder form, dissolved in dimethyl sulfoxide (DMSO) (Sigma-Aldrich) and stored at -20°C . For analysis, they were thawed and vortexed thoroughly before dilution for experiments.

Table 2.1 shows the provider's identification number, the molar mass and the stock concentration to which the compounds were diluted. For easier handling, compounds were given labels that can be obtained from these tables as well (1st generation compounds: A – T, 2nd generation compounds APU – STU).

Table 2.1: Summary of 1st and 2nd generation compounds.

Label	Provider-ID	molar mass (g mol ⁻¹)	stock concentration (mol L ⁻¹)
A	Z86135489	258.36	0.100
B	Z740776016	343.51	0.100
C	Z64811594	479.62	0.100
D	Z432791734	207.31	0.100
E	Z432388384	421.56	0.100
F	Z400358214	410.51	0.100
G	Z30159011	444.53	0.100
H	Z29313161	481.61	0.100
I	Z28039465	395.54	0.050
J	Z238035840	439.57	0.050
K	Z235988034	432.49	0.100
L	Z235983168	419.48	0.100
M	Z235975332	437.53	0.100
N	Z235972546	496.02	0.100
O	Z197898586	371.93	0.100
P	Z196790666	275.39	0.100
Q	Z190145714	460.54	0.100
R	Z123861406	203.28	0.100
S	Z1139725383	273.37	0.100
T	Z109022820	411.52	0.100
APU	Amb9790606	356.34	0.100
BRT	OSSL_298254	451.43	0.100
BUR	7969162	453.00	0.025
FLD	4464-1021	449.51	0.100
GPA	Amb9805036	340.33	0.050
HMR	OSSL_293390	361.78	0.100
ITY	AN-329/41290765	390.40	0.100
KRY	NRB00349	390.35	0.100
LSA	STK079181	414.42	0.100
MGI	STK084621	366.41	0.025
MHS	Amb4120128	326.30	0.100
MOE	PB340293238	367.32	0.010
MRG	OSSL_293422	333.29	0.100
RLF	Amb9794462	402.36	0.100
SCY	AN-329/14723078	382.42	0.100
STU	Z2239055646	489.30	0.100

2.2 In vitro screening assay with recombinant neuroserpin

To test 1st and 2nd generation compounds *in vitro*, commercially acquired full-length recombinant NS^{WT} and NS^{G392E} produced in E.coli (Biomatik) was mixed with compounds and heated for 16 hours at 37 °C in a T100 Thermal Cycler (Biorad).

The solution consisted of 5.48 μM NS and a compound in 100-fold molar excess (548 μM). Table 2.2 shows the composition the 8 μL reaction solution. To reduce pipetting mistakes, 10 \times stock solutions of compounds diluted in Dulbecco’s Phosphate-buffered saline (PBS) (Life Technologies) were prepared and stored at $-20\text{ }^{\circ}\text{C}$.

Table 2.2: Reaction solution for *in vitro* screening

	concentration (μM)	reaction volume (μL)
recombinant NS (8.76 μM)	5.48	5.000
Compound (10 mM)	547.62	0.438
PBS		2.562

As control, DMSO was used instead of a compound. An aliquot was directly stored at $-20\text{ }^{\circ}\text{C}$ after pipetting in order to avoid polymer formation (negative control). An identical DMSO reaction was heated together with the reactions containing the compounds and this served as positive control for polymerization. The experiment was repeated three and four times for 1st and 2nd generation compounds, respectively.

After heating, the probes were separated by native PAGE as described below (section 2.4). The gels were then washed with ddH₂O for 5 min and stained with GelCodeTM Blue Stain Reagent (Thermo ScientificTM) for 60 min according to the manufacturer’s protocol. Intensities of monomer, dimer and polymer bands were measured with a $\mu\text{Quant}^{\text{TM}}$ spectrophotometer (BioTek).

2.3 Cell culture

For *in vivo* screening experiments, human embryonic kidney (HEK)-293-cells stably transfected with NS^{WT} and NS^{G392E} were used (Schipanski et al., 2014). The cells were kept in a humidified incubator at 37 °C and 5% CO₂ and were handled under sterile conditions.

2.3.1 Compound concentrations

To determine suitable compound concentrations for in vivo screening, HEK-293-cells were plated at a concentration of 8×10^3 cells per well and grown overnight on 96-well-plates Dulbecco's Modified Eagle Medium (DMEM)(GibcoTM) containing 10 % fetal bovine serum (FBS) (Thermo Fisher) and 0.5 g L^{-1} Geneticin (G418-BC) (30.000 U/ml, Biochrom). The next day, the medium was discarded and exchanged with DMEM-10%-FBS-Geneticin containing 1st generation compounds at varying concentrations (1 mM, 500 μM , 200 μM , 100 μM and 50 μM). After 16 hours, cell viability was observed under a light microscope with 400 \times magnification.

Table 2.3: Compound concentrations

	examined concentrations in proliferation assay (μM)	concentration used in cell culture screening experiment (μM)
A	100, 50	100
B	100, 50	100
C	50, 10	10
D	100, 50	100
E	100, 50	100
F	2, 0.4	2
G	100, 50	100
H	100, 50	50
I	50, 10, 2	2
J	50, 10, 2	50
K	100, 50	100
L	100, 50	50
M	10, 2	10
N	50, 10, 2	2
O	100, 50	50
P	100, 50	50
Q	50, 10, 2	50
R	50, 10, 2	10
S	50, 10, 2	10
T	10, 2	2

To obtain a more precise information about the compound concentration that can be administered to HEK-293-cells without toxicity, we performed a 3-(4,5-dimethylthiazol-2-yl)-2,5-diphenyltetrazolium bromide (MTT) assay. HEK-293-cells were plated at a concentration of 8×10^3 cells per well and incubated overnight on

96-well-plates as described above. The next day, they were treated with compounds at concentrations estimated to be non-toxic by light microscopy evaluation. The examined concentrations can be obtained from Table 2.3. Four technical replicates were performed for every compound concentration. After overnight incubation, viable cells were quantified using the CellTiter 96[®] Non-Radioactive Proliferation Assay by Promega, a commercially available standardized MTT test kit. The kit’s chemicals were applied according to the manufacturer’s protocol and absorption was measured using a μ Quant[™] spectrophotometer (BioTek). As a control, the same volume of DMSO was administered to cells.

2.3.2 Screening experiment

For compound screening, HEK-293-cells were plated at a concentration of 3.5×10^5 cells per well and grown overnight in 6-well-plates with 2 mL DMEM containing 10% FBS and 0.5 g L^{-1} G418-BC. After overnight incubation, medium was discarded and replaced with a treatment medium composed of 2 mL Opti-MEM (Gibco[™]) and 2 mL 1st generation compound dissolved in DMSO. As a control, cells were treated with Opti-MEM containing the same volume of DMSO only. The treatment concentrations are listed in Table 2.3.

The next day, media were collected, centrifuged at $16 \times g$ for 10 min at 4°C and the supernatant stored at -20°C until further analysis. Remaining cells were washed with PBS. 100 μL of lysis buffer was added (see Table 2.4). Cells were scraped off using a cell scraper, vortexed and stored on ice for 10 min. The solution was centrifuged at $16 \times g$ for 10 min at 4°C and the cell extract stored at -20°C until further analysis.

Table 2.4: Composition of the lysis buffer

cOmplete [™] Protease Inhibitor Cocktail (Roche)	1X
Triton X-100 (Roth)	1 %
NaCl (Th.Geyer)	150 mM
Tris (Sigma) pH 7.5	20 mM

2.3.3 Immunocytochemistry

For immunocytochemistry imaging, HEK-293-cells were plated at a concentration of 7×10^4 and grown overnight on glass coverslips in 24-well-plates as described above. The next day, media were discarded and the coverslips were washed two consecutive times with PBS. The cells were then fixed with a solution consisting

of 4% paraformaldehyde (Merck) dissolved in PBS for 15 min at room temperature. The fixed cells were washed three times for 5 min in PBS. To minimize un-specific antibody binding, a blocking solution was applied to the cells for 60 min (Table 2.5). Then, the primary antibody (anti-NS ab33077 (rabbit), 1:100, abcam), diluted in antibody incubation solution Table 2.6, was applied for 60 min. After another PBS-washing-cycle, the secondary anti-rabbit antibody conjugated with fluorescent Alexa 488 (anti-rabbit Alexa Fluor[®] 488 (donkey), 1:500, Life Technologies) was incubated for 30 min in the dark. The cells were washed in PBS again, and coverslips were mounted on plates with Fluoromount-G (Southern Biotech) containing 4',6-diamidino-2-phenylindole (DAPI) and stored in the dark until further analysis. Immunocytochemical imaging was conducted with a Leica TCS SP5 confocal microscope.

Table 2.5: Composition of blocking solution

FCS	10.0 %
Glycine	0.1 %
Saponin	0.1 %
in PBS	

Table 2.6: Composition of antibody incubation solution

FCS	1.0 %
Glycine	0.1 %
Saponin	0.1 %
in PBS	

2.4 Polyacrylamide gel electrophoresis

For PAGE experiments, native or SDS (8%) acrylamide gels with either 10 or 15 wells were prepared one day prior to the experiment and stored at 4 °C (Table 2.7 to Table 2.10).

For SDS-PAGE experiments, running buffer composition can be obtained from Table 2.11. Native PAGE was carried out in anode and cathode buffer (Table 2.12). A pre-run for 10 min at 100 V in running buffer was carried out. Running buffers were replaced with fresh ones before loading of probes.

In the *in vitro* experiment with recombinant NS, the 8 μ L reaction solution was diluted to 40 μ L with 22 μ L ddH₂O and 10 μ L 4 \times native loading buffer (Table 2.13).

Table 2.7: Composition of native running gel

30 % Acrylamide	5 mL
ddH ₂ O	6.37 mL
1 M Tris pH 7.8	7.12 mL
10 % Ammonium persulfate (APS)	187.5 μ L
Tetramethylethylenediamine (TEMED)	7.5 μ L

Table 2.8: Composition of native stacking gel

30 % Acrylamide	1.3 mL
ddH ₂ O	6 mL
1 M Tris pH 7.8	500 μ L
10 % APS	80 μ L
TEMED	8 μ L

For the *in vivo* experiment, 30 μ L of either cell extract or supernatant were mixed with 10 μ L of 4 \times native loading buffer and loaded to the gels. First lane of every gel contained native marker (NativeMarkTM, InvitrogenTM). Gels were run at 100 V for approximately 95 min.

Table 2.9: Composition of SDS running gel

30 % Acrylamide	6.6 mL
ddH ₂ O	8.2 mL
4 \times Running Gel Buffer	5 mL
10 % APS	200 μ L
TEMED	8 μ L

SDS-PAGE was carried out in a similar manner. Prior to the loading, the probes were mixed with SDS loading buffer and heated at 95 $^{\circ}$ C for 5 min (Table 2.13).

Table 2.10: Composition of SDS stacking gel

30 % Acrylamide	1.35 mL
ddH ₂ O	6.2 mL
4× Stacking Gel Buffer	2.5 mL
10 % APS	30 μ L
TEMED	20 μ L

2.5 Western Blotting

Western blotting was done on nitrocellulose membranes (0.2 μ m, BioRad) at 100 V for 60 min in either native or SDS transfer buffer (Table 2.14).

Table 2.11: Composition of 10X native running buffer

Tris	250 mM
Glycine	1.92 M
SDS	1 %

Table 2.12: Composition of 10X native running buffer

	Cathode	Anode
Tris	0.53 M	0.1 M
pH	8.9	7.8
Glycine	0.68 M	0.68 M

To reveal the native marker bands, the membranes were stained with Ponceau S (Sigma-Aldrich) and bands were marked with a pencil. To investigate NS polymers and protein disulfide isomerase (PDI) as a housekeeping protein simultaneously, the cell extract membranes were cut horizontally just above the 146 kDa marker band.

Membranes were then blocked for 60 min with a solution containing 5 % nonfat dry milk (Frema reform) in Tris-buffered saline with Tween 20 (TBST) (Table 2.15). Milk-TBST-solution was discarded and replaced with a fresh solution containing antibodies against NS (1:1000, ab32901, goat, abcam) and PDI (1:5000, anti-PDI, rabbit, StressMarq Biosciences). The antibodies were incubated overnight on a shaker at 4 °C.

The next day, membranes were washed three times for 5 min with TBST before administering the secondary anti-bodies (anti-goat [1:5000] and anti-rabbit [1:5000] both coupled to horseradish peroxidase) in milk-TBST-solution for 60 min. After

Table 2.13: Composition of 4× loading buffer

	Native	SDS
Glycerol	40 % (v/v)	40 % (v/v)
Tris pH 6.8	250 mM	200 mM
Bromophenol blue	0.4 % (w/v)	0.4 % (w/v)
SDS		8 % (w/v)

Table 2.14: Composition of Western Blot transfer buffer

	native	SDS
10× Buffer	10 % (v/v)	10 % (v/v)
Tris pH 8.3	250 mM	
Glycine	1.92 M	
ddH ₂ O	90 % (v/v)	70 % (v/v)
Methanol		20 % (v/v)

a second wash cycle with TBST, a 1:2 mixture of SuperSignalTM West Pico and SuperSignalTM West Femto (Thermo Scientific) was applied for 5 min. Bands were visualized with ChemiDoc XRS and Quantity One software (BioRad).

Table 2.15: Composition of TBST

Tris pH 8.0	10 mM
NaCl	150 mM
Tween 20	0.05 %

2.6 Statistical analysis

In the *in vitro* screening assay with recombinant NS, intensities (I) of monomer, dimer and polymer bands were normalized to the total intensity of the corresponding lane.

$$x_{\text{monomers}} = \frac{I_{\text{monomers}}}{I_{\text{monomers}} + I_{\text{dimers}} + I_{\text{polymers}}}$$

$$x_{\text{dimers}} = \frac{I_{\text{dimers}}}{I_{\text{monomers}} + I_{\text{dimers}} + I_{\text{polymers}}}$$

$$x_{\text{polymers}} = \frac{I_{\text{polymers}}}{I_{\text{monomers}} + I_{\text{dimers}} + I_{\text{polymers}}}$$

In the cell culture screening assay, intensities of polymers only were measured and normalized to the PDI signal.

$$x_{\text{cell extract}} = \frac{I_{\text{cell extract}}}{I_{\text{PDI}}}$$

$$x_{\text{supernatant}} = \frac{I_{\text{supernatant}}}{I_{\text{PDI}}}$$

Data are reported as average \pm standard deviation (\pm SD). For *in vitro* experiments, the total amount of protein per lane was set to 1. In the cell culture assay, band intensity of the DMSO control was set to 1. For null hypothesis testing, a two-sided unpaired Student's t-test was used with the heated (positive) DMSO controls as reference groups.

All statistical analysis was performed using the programming language R (version 3.6.1) in RStudio (version 1.2.1335).

3 Results

3.1 In vitro screening assay with recombinant neuroserpin

Two virtual screening assays were performed to select compounds with high binding affinity to the β -sheet A of NS from large libraries of commercially available small chemicals. By binding to NS, the compounds should prevent polymerization of mutant NS in FENIB. Compounds of the first and second virtual screening are termed 1st and 2nd generation compounds, respectively.

To test the anti-polymerization activity of these compounds *in vitro*, a screening assay was designed using recombinant NS^{WT} and NS^{G392E}, a mutation leading to a severe form of FENIB. NS was mixed with a compound and incubated at a temperature of 37 °C for 16 hours. The NS solution was then separated by non-denaturing PAGE and stained with Coomassie-blue (Figure 3.1 to Figure 3.7).

NS separates into different bands. NS^{WT} previously mixed with DMSO — the solvent used to dissolve the compounds — was directly loaded on the gel and consists mainly of monomers (m) and small traces of dimers (d) (first lane, DMSO sample). As a control for polymerization, NS^{WT} was mixed with DMSO and heated as the NS-compound samples (second lane, DMSO⁺). In consequence, the monomer band was weaker, more dimers were present and bands consisting of high molecular weight polymers (p) became apparent. The band pattern observed for NS^{WT} incubated with compounds was very similar to the one observed for the DMSO⁺ sample, although small variations in band intensity were apparent (e.g. incubation of NS^{WT} with compound BUR, Figure 3.4 to Figure 3.7).

In contrast to NS^{WT}, NS^{G392E} exhibited all three species (monomers, dimers and polymers) before being incubated. The band pattern unaltered upon incubation with DMSO or compounds.

The intensities of monomer, dimer and polymer bands were measured separately and put in proportion to the total sum of intensities per lane. Values from the different technical replicates were averaged (1st generation: $n = 3$, 2nd generation: $n = 4$). Significant changes of treatment groups to DMSO⁺ control were tested using a two-sided student's t-test (Table 3.1 to Table 3.4 and Figure 3.8 to Figure 3.9).

A significant reduction of NS^{WT} polymers from 0.54 ± 0.07 to 0.39 ± 0.05 ($p = 0.0032$) can be achieved by treatment with compound BUR. Moreover, treatment with BUR results in a significant increase in dimers from 0.22 ± 0.04 to 0.32 ± 0.06 ($p = 0.0358$). Although not significantly, the amount of monomers showed a tendency towards increment as well from 0.24 ± 0.05 to 0.29 ± 0.05 ($p = 0.1037$).

Two significant results were achieved for NS^{G392E}: A decrease in dimers from 0.20 ± 0.03 to 0.14 ± 0.02 ($p = 0.0367$) after treatment with compound FLD and an increase of NS^{G392E} polymers from 0.70 ± 0.04 to 0.78 ± 0.03 ($p = 0.0450$) after treatment with compound O. The other compounds do not seem to significantly affect the distribution of recombinant NS species.

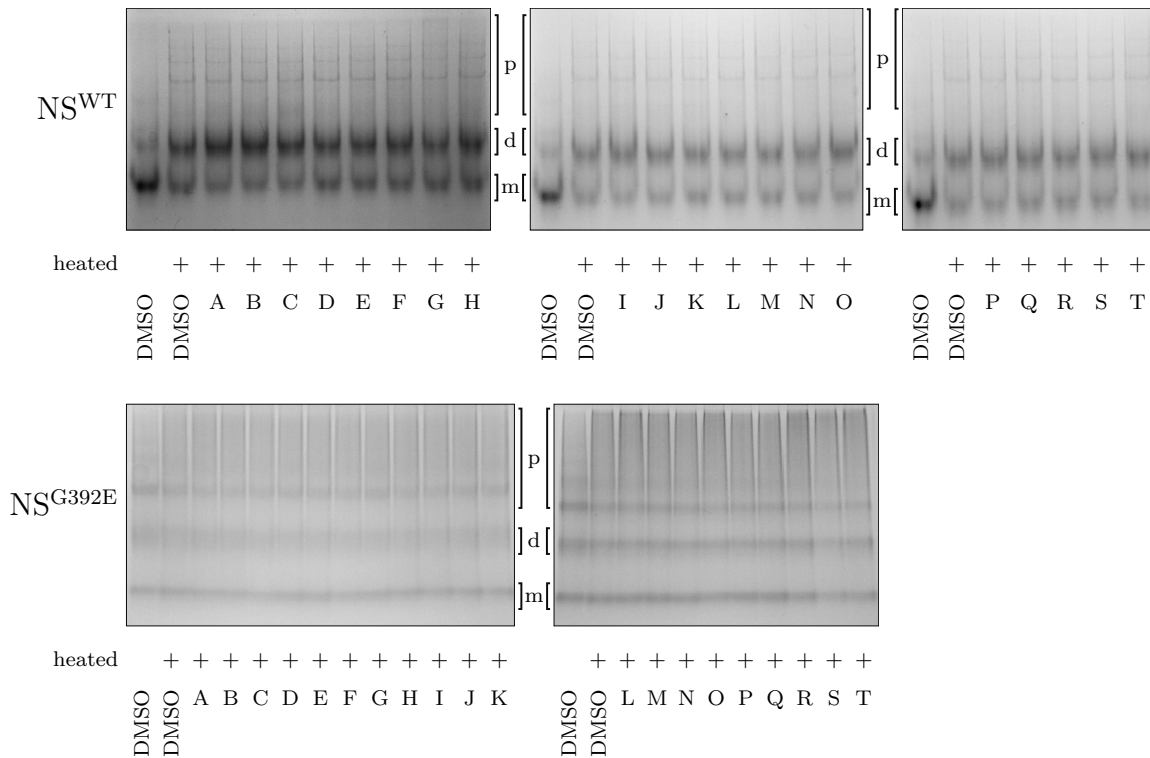


Figure 3.1: *In vitro* analysis of 1st generation compounds (set 1 of 3). Recombinant NS^{WT} (upper row) or NS^{G392E} (lower row) and a 1st generation compound (A-T, dissolved in DMSO) were mixed with PBS and heated at 37 °C for 16 hours. The NS species were separated by non-denatured PAGE and stained with Coomassie blue. First and second lane of every gel contain controls of NS mixed with DMSO only before and after incubation, respectively. Bands corresponding to monomers (m), dimers (d) and polymers (p) are labeled accordingly.

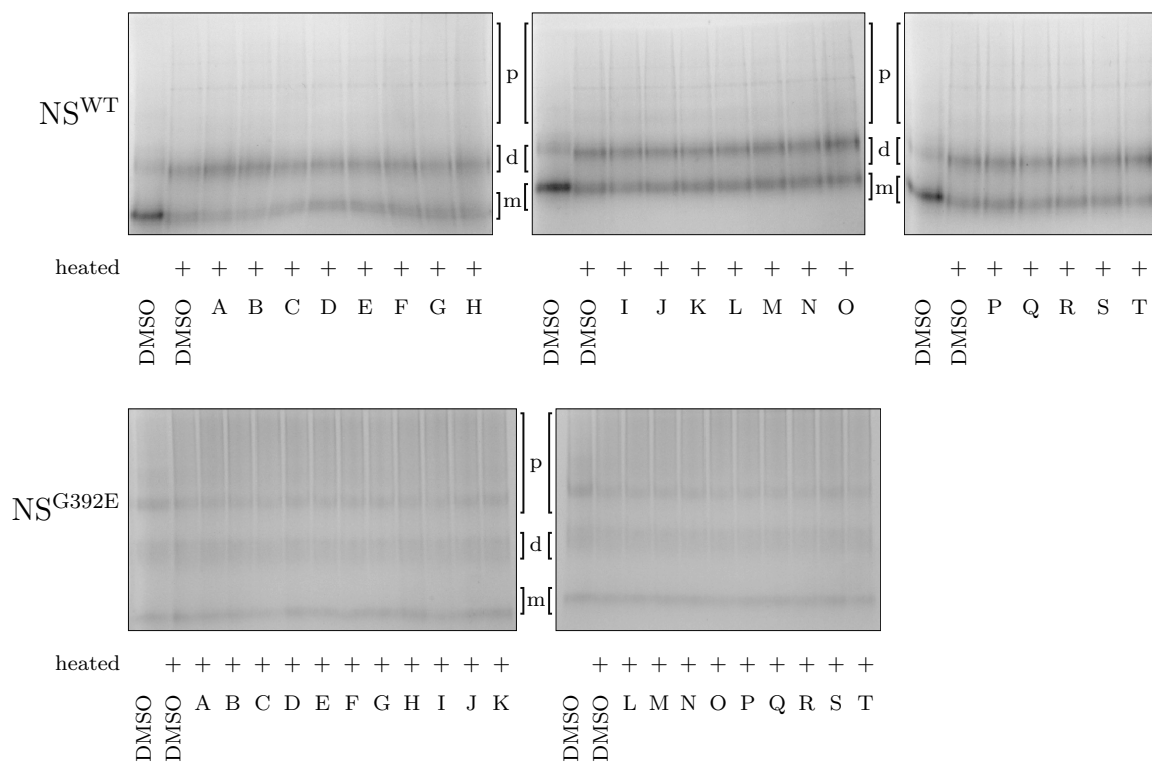


Figure 3.2: *In vitro* analysis of 1st generation compounds (set 2 of 3). Recombinant NS^{WT} (upper row) or NS^{G392E} (lower row) and a 1st generation compound (A-T, dissolved in DMSO) were mixed with PBS and heated at 37 °C for 16 hours. The NS species were separated by non-denatured PAGE and stained with Coomassie blue. First and second lane of every gel contain controls of NS mixed with DMSO only before and after incubation, respectively. Bands corresponding to monomers (m), dimers (d) and polymers (p) are labeled accordingly.

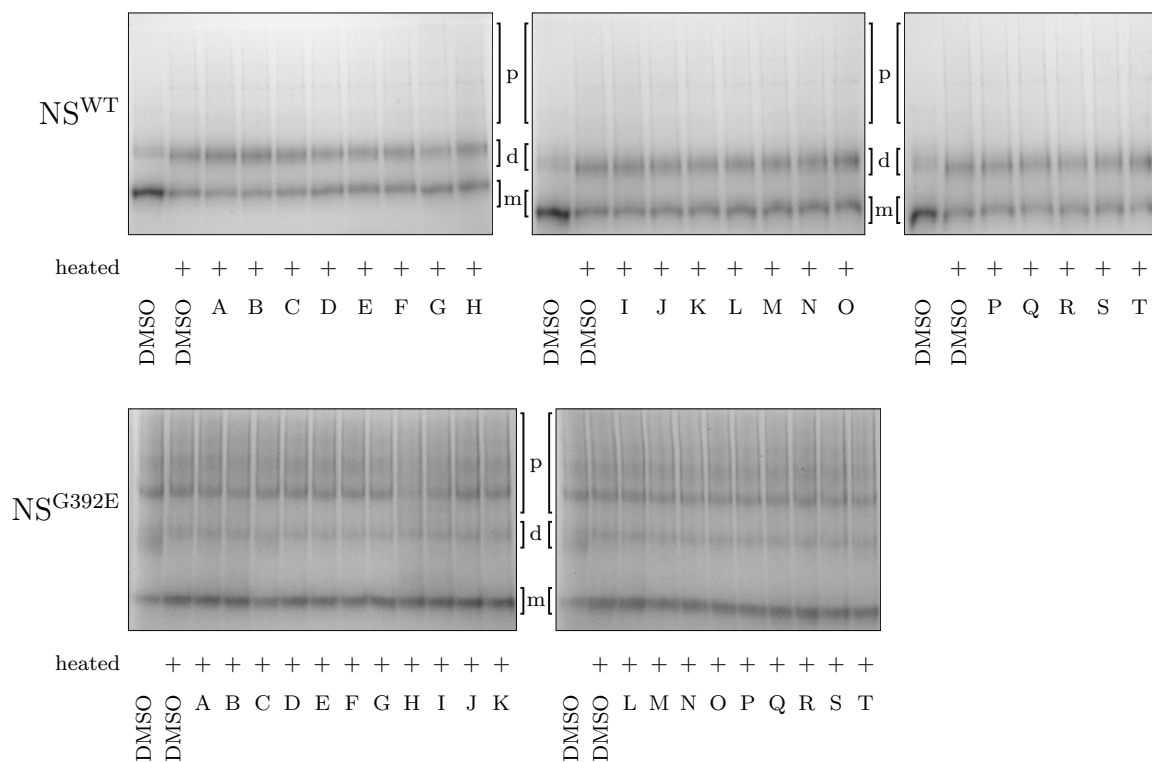


Figure 3.3: *In vitro* analysis of 1st generation compounds (set 3 of 3). Recombinant NS^{WT} (upper row) or NS^{G392E} (lower row) and a 1st generation compound (A-T, dissolved in DMSO) were mixed with PBS and heated at 37°C for 16 hours. The NS species were separated by non-denatured PAGE and stained with Coomassie blue. First and second lane of every gel contain controls of NS mixed with DMSO only before and after incubation, respectively. Bands corresponding to monomers (m), dimers (d) and polymers (p) are labeled accordingly.

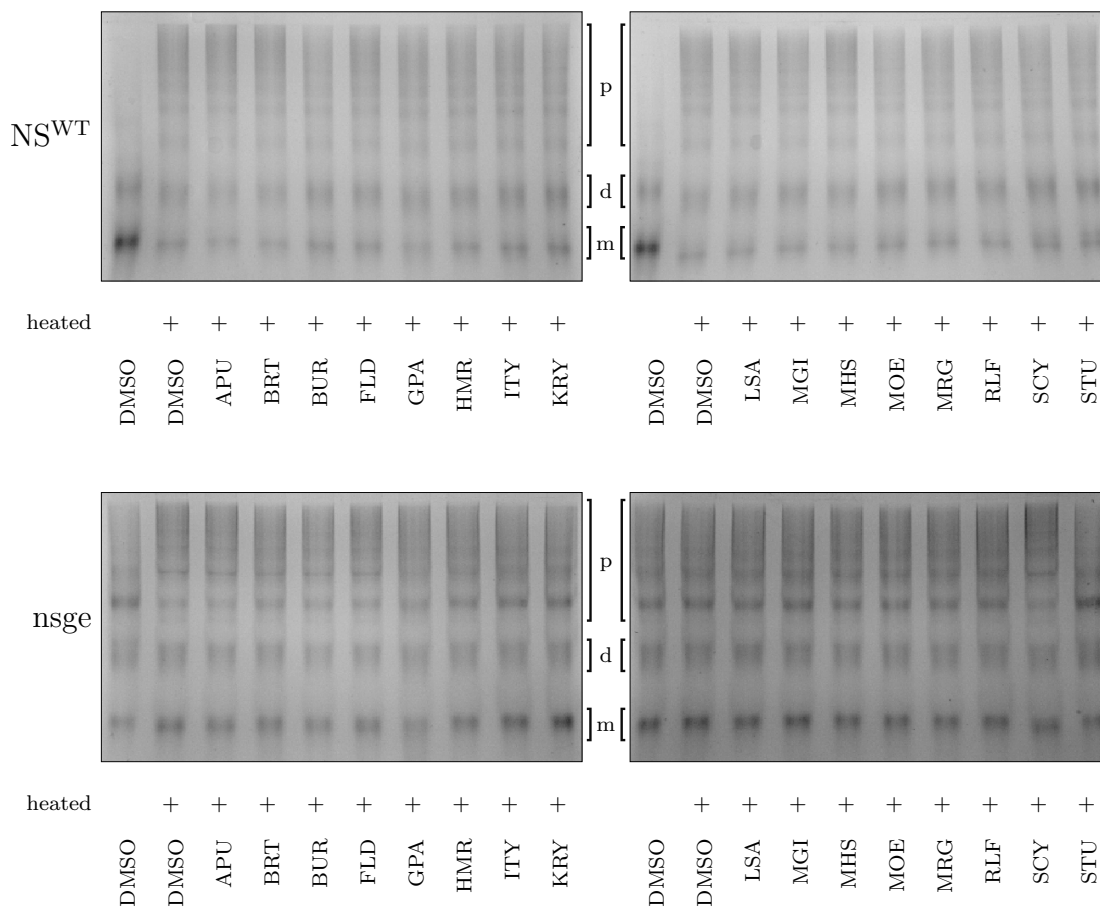


Figure 3.4: *In vitro* analysis of 2nd generation compounds (set 1 of 4). Recombinant NS^{WT} (upper row) or NS^{G392E} (lower row) and a 2nd generation compound (APU-STU, dissolved in DMSO) were mixed with PBS and heated at 37 °C for 16 hours. The NS species were separated by non-denatured PAGE and stained with Coomassie blue. First and second lane of every gel contain controls of NS mixed with DMSO only before and after incubation, respectively. Bands corresponding to monomers (m), dimers (d) and polymers (p) are labeled accordingly.

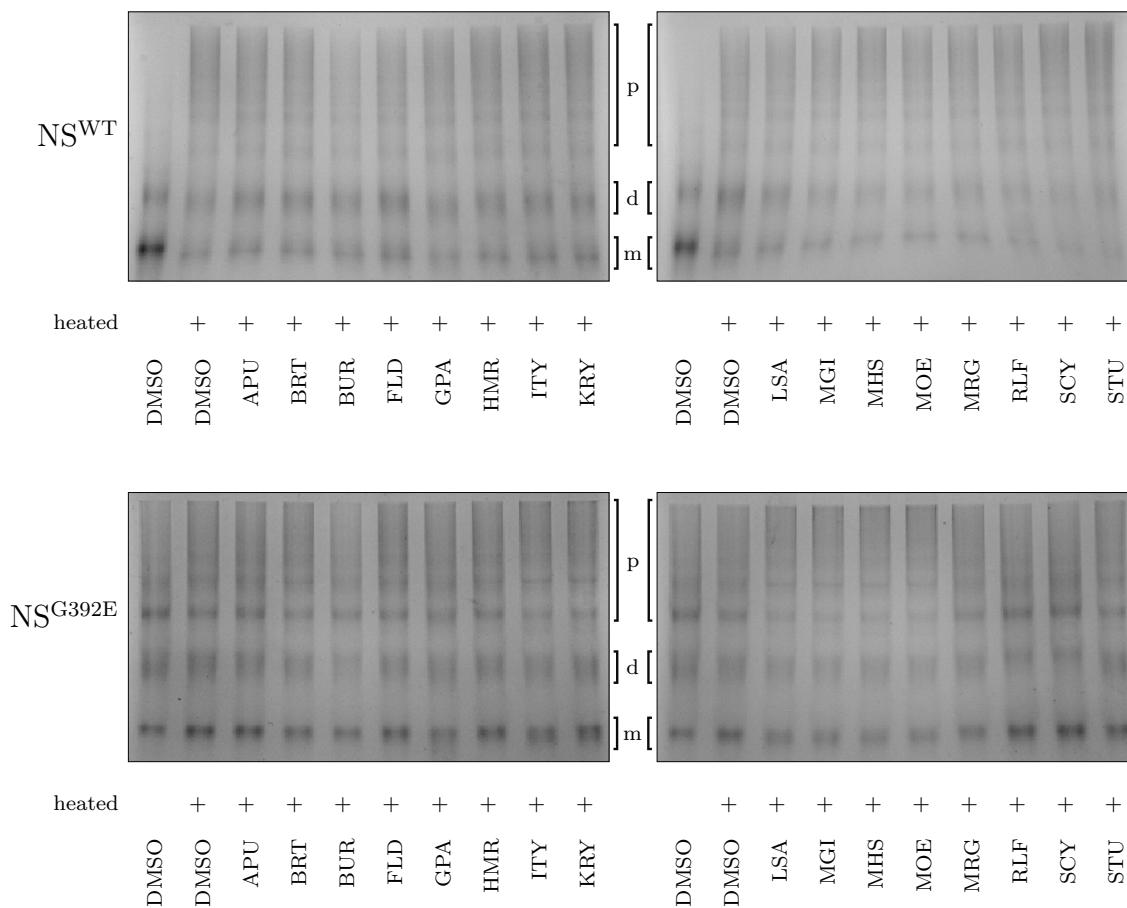


Figure 3.5: *In vitro* analysis of 2nd generation compounds (set 2 of 4). Recombinant NS^{WT} (upper row) or NS^{G392E} (lower row) and a 2nd generation compound (APU-STU, dissolved in DMSO) were mixed with PBS and heated at 37 °C for 16 hours. The NS species were separated by non-denatured PAGE and stained with Coomassie blue. First and second lane of every gel contain controls of NS mixed with DMSO only before and after incubation, respectively. Bands corresponding to monomers (m), dimers (d) and polymers (p) are labeled accordingly.

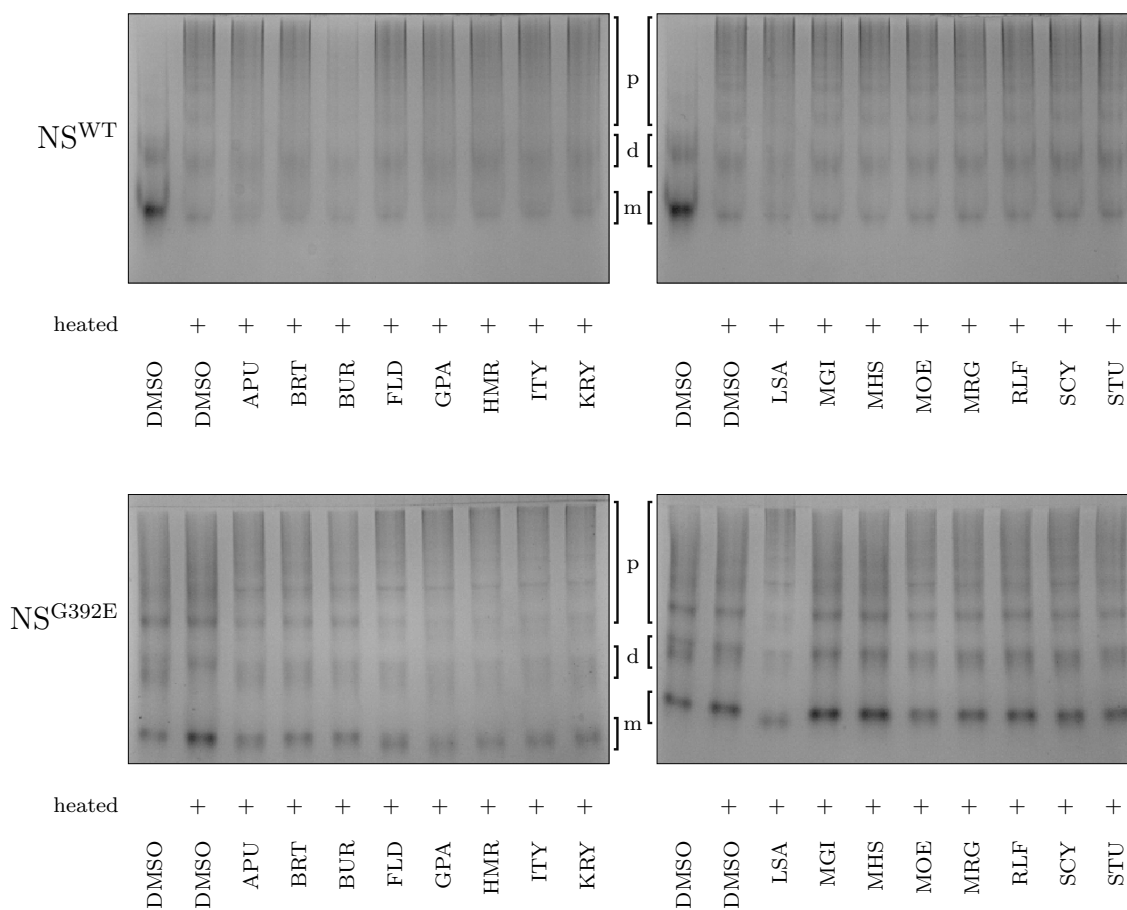


Figure 3.6: *In vitro* analysis of 2nd generation compounds (set 3 of 4). Recombinant NS^{WT} (upper row) or NS^{G392E} (lower row) and a 2nd generation compound (APU-STU, dissolved in DMSO) were mixed with PBS and heated at 37 °C for 16 hours. The NS species were separated by non-denatured PAGE and stained with Coomassie blue. First and second lane of every gel contain controls of NS mixed with DMSO only before and after incubation, respectively. Bands corresponding to monomers (m), dimers (d) and polymers (p) are labeled accordingly.

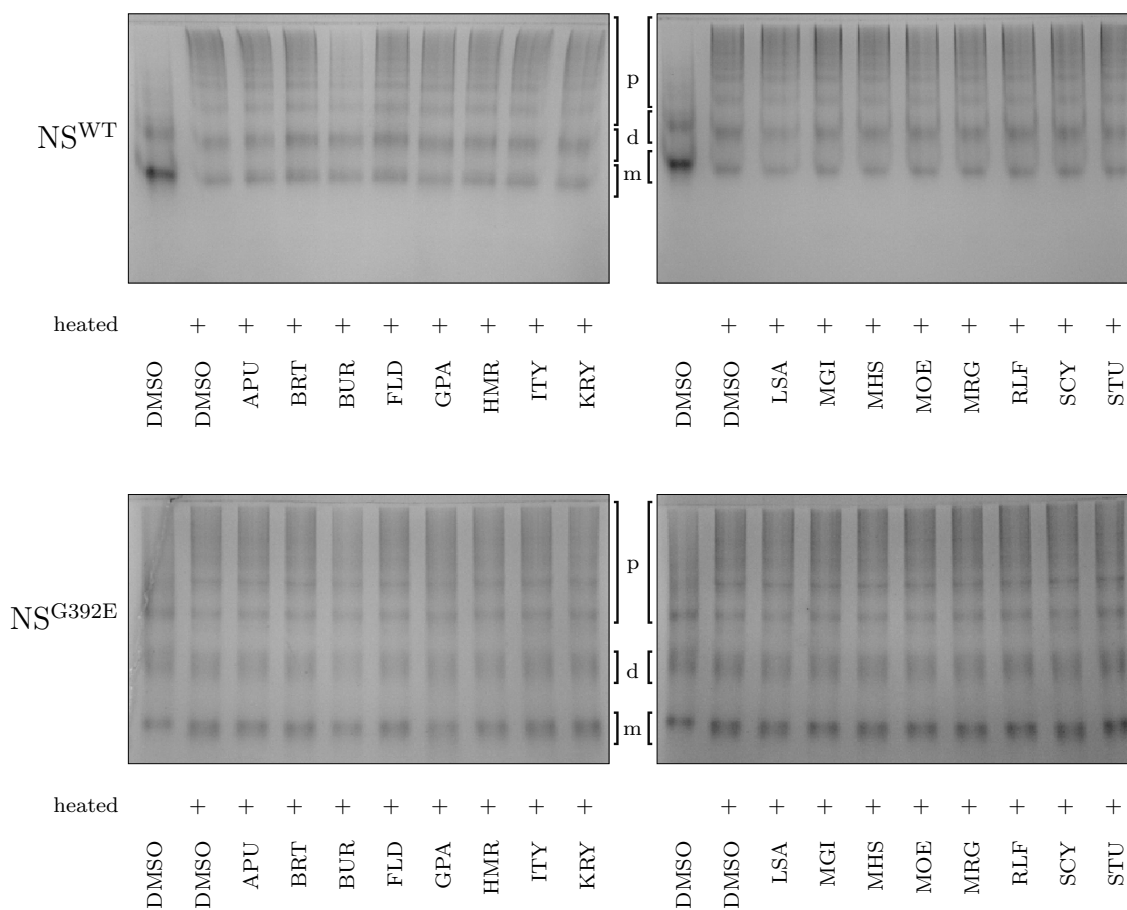


Figure 3.7: *In vitro* analysis of 2nd generation compounds (set 4 of 4). Recombinant NS^{WT} (upper row) or NS^{G392E} (lower row) and a 2nd generation compound (APU-STU, dissolved in DMSO) were mixed with PBS and heated at 37 °C for 16 hours. The NS species were separated by non-denatured PAGE and stained with Coomassie blue. First and second lane of every gel contain controls of NS mixed with DMSO only before and after incubation, respectively. Bands corresponding to monomers (m), dimers (d) and polymers (p) are labeled accordingly.

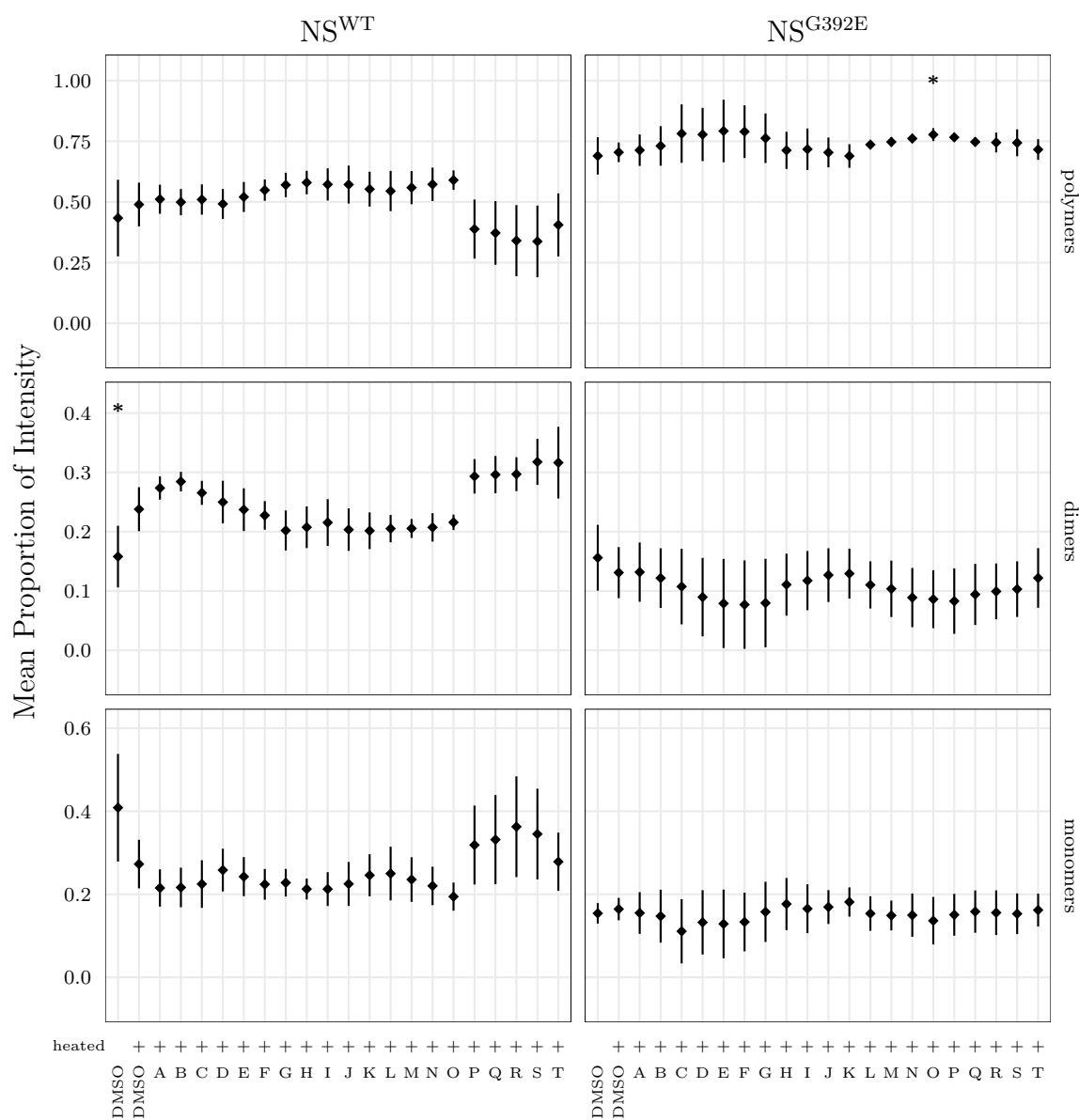


Figure 3.8: *In vitro* screening assay with 1st generation compounds (A-T). Intensities of monomers, dimers and polymers were measured and put in proportion to the total intensity of each lane. The means and standard deviations were calculated for the technical replicates and plotted for every compound. As controls NS (mixed with DMSO only) prior and after incubation were used. Asterisks indicate a significant difference to the DMSO⁺ control (* $\hat{=}$ p-value < 0.05, students t-Test).

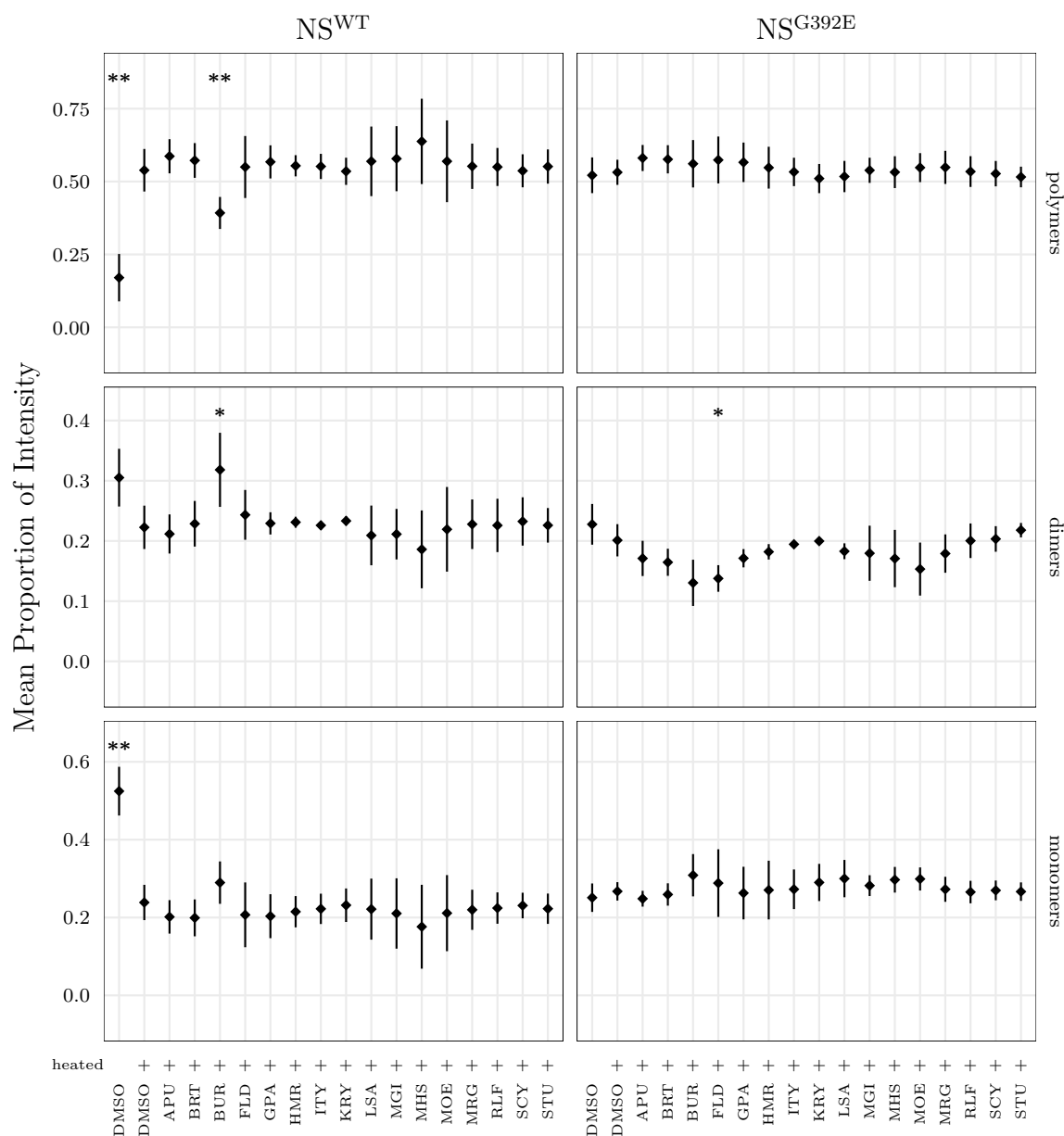


Figure 3.9: *In vitro* screening assay with 2nd generation compounds (APU-STU).

Intensities of monomers, dimers and polymers were measured and put in proportion to the total intensity of each lane. The means and standard deviations were calculated for the technical replicates and plotted for every compound. As controls NS (mixed with DMSO only) prior and after incubation were used. Asterisks indicate a significant difference to the DMSO⁺ control (* $\hat{=}$ p-value < 0.05, ** $\hat{=}$ p-value < 0.01, students t-Test).

Table 3.1: *In vitro* screening experiment with 1st generation compounds

	NS ^{WT}								
	polymers			dimers			monomers		
	mean	SD±	p-value	mean	SD±	p-value	mean	SD±	p-value
DMSO	0.43	0.16	0.4870	0.16	0.05	0.0161	0.41	0.13	0.2825
DMSO (heated)	0.49	0.09		0.24	0.04		0.27	0.06	
A	0.51	0.06	0.9556	0.27	0.02	0.1628	0.22	0.04	0.3133
B	0.50	0.05	0.8637	0.28	0.02	0.0929	0.22	0.05	0.3426
C	0.51	0.06	0.9734	0.27	0.02	0.2549	0.22	0.06	0.4975
D	0.49	0.06	0.7689	0.25	0.04	0.6602	0.26	0.05	0.9316
E	0.52	0.06	0.8242	0.24	0.04	0.9990	0.24	0.05	0.7448
F	0.55	0.04	0.4275	0.23	0.02	0.6877	0.22	0.04	0.3752
G	0.57	0.05	0.2644	0.20	0.03	0.2498	0.23	0.03	0.4128
H	0.58	0.05	0.2046	0.21	0.04	0.3299	0.21	0.03	0.2012
I	0.57	0.07	0.7211	0.22	0.04	0.6877	0.21	0.04	0.4015
J	0.57	0.08	0.7536	0.20	0.04	0.9904	0.22	0.05	0.6560
K	0.55	0.07	0.9989	0.20	0.03	0.9269	0.25	0.05	0.9546
L	0.54	0.08	0.9004	0.21	0.02	0.9447	0.25	0.06	0.8926
M	0.56	0.07	0.9087	0.21	0.02	0.9225	0.24	0.05	0.8476
N	0.57	0.07	0.7216	0.21	0.02	0.8662	0.22	0.05	0.5483
O	0.59	0.04	0.4128	0.22	0.01	0.4918	0.19	0.03	0.1832
P	0.39	0.12	0.8398	0.29	0.03	0.3883	0.32	0.10	0.9856
Q	0.37	0.13	0.7264	0.30	0.03	0.3563	0.33	0.11	0.8848
R	0.34	0.15	0.5464	0.30	0.03	0.3145	0.36	0.12	0.6346
S	0.34	0.15	0.5312	0.32	0.04	0.1754	0.35	0.11	0.7592
T	0.41	0.13	0.9846	0.32	0.06	0.3407	0.28	0.07	0.5182

Table 3.2: *In vitro* screening experiment with 1st generation compounds

NS ^{G392E}									
	polymers			dimers			monomers		
	mean	SD±	p-value	mean	SD±	p-value	mean	SD±	p-value
DMSO	0.69	0.08	0.4989	0.16	0.06	0.5042	0.15	0.02	0.8073
DMSO (heated)	0.70	0.04		0.13	0.04		0.16	0.03	
A	0.71	0.06	0.7610	0.13	0.05	0.9457	0.15	0.05	0.7288
B	0.73	0.08	0.5888	0.12	0.05	0.7682	0.15	0.06	0.6520
C	0.78	0.12	0.3547	0.11	0.06	0.5942	0.11	0.08	0.3325
D	0.78	0.11	0.3384	0.09	0.07	0.4056	0.13	0.08	0.5222
E	0.79	0.13	0.3321	0.08	0.08	0.3548	0.13	0.08	0.5064
F	0.79	0.11	0.2809	0.08	0.07	0.3379	0.13	0.07	0.4997
G	0.76	0.10	0.3994	0.08	0.07	0.3584	0.16	0.07	0.8369
H	0.71	0.08	0.7906	0.11	0.05	0.5989	0.18	0.06	0.8488
I	0.72	0.09	0.7523	0.12	0.05	0.6970	0.17	0.06	0.9465
J	0.70	0.06	0.8935	0.13	0.05	0.8485	0.17	0.04	0.9698
K	0.69	0.05	0.8636	0.13	0.04	0.8922	0.18	0.04	0.6594
L	0.74	0.02	0.2932	0.11	0.04	0.6489	0.15	0.04	0.8154
M	0.75	0.02	0.1627	0.10	0.05	0.5647	0.15	0.04	0.6707
N	0.76	0.02	0.0773	0.09	0.05	0.3772	0.15	0.05	0.7653
O	0.78	0.03	0.0450	0.09	0.05	0.3424	0.14	0.06	0.5519
P	0.77	0.01	0.0633	0.08	0.06	0.3424	0.15	0.05	0.7789
Q	0.75	0.02	0.1585	0.09	0.05	0.4489	0.16	0.05	0.9468
R	0.74	0.04	0.3244	0.10	0.05	0.4968	0.16	0.05	0.8934
S	0.74	0.06	0.4451	0.10	0.05	0.5539	0.15	0.05	0.8274
T	0.72	0.04	0.9023	0.12	0.05	0.8993	0.16	0.04	0.9643

Table 3.3: *In vitro* screening experiment with 2nd generation compounds

	NSWT								
	polymers			dimers			monomers		
	mean	SD±	p-value	mean	SD±	p-value	mean	SD±	p-value
DMSO	0.17	0.08	0.0025	0.31	0.05	0.1202	0.52	0.06	0.0021
DMSO (heated)	0.54	0.07		0.22	0.04		0.24	0.05	
APU	0.59	0.06	0.5318	0.21	0.03	0.9788	0.20	0.04	0.3923
BRT	0.57	0.06	0.7987	0.23	0.04	0.4433	0.20	0.05	0.3801
BUR	0.39	0.05	0.0032	0.32	0.06	0.0358	0.29	0.05	0.1037
FLD	0.55	0.11	0.8365	0.24	0.04	0.2222	0.21	0.08	0.6836
GPA	0.57	0.06	0.8951	0.23	0.02	0.1924	0.20	0.06	0.5103
HMR	0.55	0.04	0.7762	0.23	0.01	0.0889	0.21	0.04	0.6682
ITY	0.55	0.04	0.7404	0.23	0.01	0.1698	0.22	0.04	0.8727
KRY	0.54	0.05	0.4239	0.23	0.01	0.0659	0.23	0.04	0.8546
LSA	0.57	0.12	0.5051	0.21	0.05	0.5008	0.22	0.08	0.5726
MGI	0.58	0.11	0.4221	0.21	0.04	0.5056	0.21	0.09	0.4854
MHS	0.64	0.15	0.2173	0.19	0.06	0.2833	0.18	0.11	0.2824
MOE	0.57	0.14	0.5477	0.22	0.07	0.7425	0.21	0.10	0.5186
MRG	0.55	0.08	0.5663	0.23	0.04	0.8489	0.22	0.05	0.4568
RLF	0.55	0.07	0.5704	0.23	0.04	0.8090	0.22	0.04	0.4858
SCY	0.54	0.06	0.7110	0.23	0.04	0.9578	0.23	0.03	0.5774
STU	0.55	0.06	0.5436	0.23	0.03	0.7853	0.22	0.04	0.4556

Table 3.4: *In vitro* screening experiment with 2nd generation compounds

NSG392E									
	polymers			dimers			monomers		
	mean	SD±	p-value	mean	SD±	p-value	mean	SD±	p-value
DMSO	0.52	0.06	0.5604	0.23	0.03	0.3122	0.25	0.04	0.6686
DMSO (heated)	0.53	0.04		0.20	0.03		0.27	0.02	
APU	0.58	0.04	0.4388	0.17	0.03	0.4045	0.25	0.02	0.6955
BRT	0.58	0.05	0.5426	0.16	0.02	0.2346	0.26	0.03	0.7424
BUR	0.56	0.08	0.9231	0.13	0.04	0.0536	0.31	0.05	0.1331
FLD	0.57	0.08	0.7117	0.14	0.02	0.0367	0.29	0.09	0.4838
GPA	0.57	0.07	0.8163	0.17	0.02	0.3310	0.26	0.07	0.8035
HMR	0.55	0.07	0.8369	0.18	0.01	0.6506	0.27	0.08	0.6857
ITY	0.53	0.05	0.4779	0.19	0.00	0.7988	0.27	0.05	0.5168
KRY	0.51	0.05	0.1949	0.20	0.01	0.5818	0.29	0.05	0.2257
LSA	0.52	0.05	0.7627	0.18	0.01	0.0544	0.30	0.05	0.5128
MGI	0.54	0.04	0.3029	0.18	0.05	0.2601	0.28	0.03	0.9582
MHS	0.53	0.05	0.4723	0.17	0.05	0.1838	0.30	0.03	0.4626
MOE	0.55	0.05	0.2357	0.15	0.04	0.0688	0.30	0.03	0.3802
MRG	0.55	0.06	0.2693	0.18	0.03	0.1375	0.27	0.03	0.6880
RLF	0.53	0.05	0.4283	0.20	0.03	0.5271	0.27	0.03	0.4406
SCY	0.53	0.04	0.5026	0.20	0.02	0.5664	0.27	0.03	0.5413
STU	0.52	0.04	0.7419	0.22	0.01	0.6363	0.27	0.02	0.4236

3.2 In vivo screening assay with a FENIB cell model

3.2.1 Characterization of the FENIB cell model

To screen the possible anti-polymerogenic activity of 1st generation compounds in a cell model of FENIB, experiments were designed with stably transfected HEK-293-cells overexpressing NS^{G392E} (NS^{G392E}-cells).

First, NS^{G392E} expression was characterized in stably transfected HEK-293-cells and compared to HEK-293-cells stably overexpressing NS^{WT}. Both cell lines (NS^{WT} and NS^{G392E}) were seeded in culture plates and incubated overnight. Cell extract and supernatant were collected and separated using SDS and non-denaturing PAGE. After Western Blot transfer, the membrane was probed with an antibody recognizing NS (Figure 3.10, A and B). In SDS-PAGE, NS^{WT} can be found in the cell extract (CE) as well as the supernatant (SN) of the medium as a single band at approximately 45 kDa (Figure 3.10, A). NS^{G392E} appears only in cell extract, no band is observed in the medium.

Similar to SDS-PAGE, a strong band representing NS^{WT} monomers is found in cell extract and faintly in supernatant as well (Figure 3.10, B). Moreover, a smear of high molecular weight aggregates is observed at weak intensity in the cell extract. NS^{G392E}, on the other hand, is mostly detected in high molecular weight bands in cell extract. Only a small fraction of NS^{G392E} is found as monomers. Bands of high molecular weight become apparent in the supernatant as well.

Afterwards, the subcellular distribution and ER accumulation of NS was investigated by immunohistochemistry (Figure 3.10, C and D). Again, both cell lines stably overexpressing NS^{WT} and NS^{G392E} were seeded on glass coverslips. After overnight incubation, the cells were fixed and stained with anti-NS-antibodies and DAPI as a marker of the nucleus. The green fluorescence signal of NS^{WT} appears evenly distributed throughout the cell's body in an ER-cisternae-like pattern (Figure 3.10, C). In contrast, NS^{G392E} forms punctate accumulations similar to those previously described for polymerogenic NS by Miranda et al. (2004) (Figure 3.10, D).

3.2.2 Determination of suitable concentrations of compounds for treatment

To our best knowledge, the compounds investigated in this study have not been used as treatment in live cells before. Therefore, we set out to determine a suitable concentration that is (i) high enough to have a measurable effect and (ii) not toxic to NS^{G392E}-HEK-293-cells.

First, suitable concentrations of 1st generation compounds were estimated by applying them to NS^{G392E}-cells at concentrations ranging from 50 μ M to 1 mM. Af-

ter overnight incubation, cell viability and morphology was evaluated by light microscopy (400× magnification, data not shown). All compounds appeared to be toxic at concentrations higher than 100 μM .

Based on this prior estimation, a MTT cell proliferation assay was carried out (Table 2.3). Again, compounds were administered at concentrations ranging from 0.4 μM to 100 μM and incubated on cells overnight. The assay indirectly evaluates the number of viable cells by measuring the amount of yellow MTT that is reduced to purple formazan by the cellular enzyme oxidoreductase.

As control, the same volume of DMSO (0.1%) was administered to the cells (positive control for cell viability). Moreover, we used a high dose of 10% DMSO that is toxic to HEK-293-cells and, thus, represents a negative control.

Four measurements ($n = 4$) were performed, data were averaged and the 0.1% DMSO positive control was set to 1 (Figure 3.11). A threshold of 0.8 relative to the positive control was chosen to identify viability. The lowest value was measured with the 10% DMSO negative control, proving feasibility of the assay. For the *in vivo* screening assay, the highest compound concentration with values above 0.8 relative to the DMSO positive control was used. In Table 2.1 the concentrations used in this cell model assay are summarized.

3.2.3 Screening compounds in a HEK-cell-model of FENIB

To test the compounds' ability to inhibit polymerization in a cell model of FENIB, NS^{G392E}-cells were incubated overnight in media containing the compounds in the ascertained concentrations (see Figure 3.11 and Table 2.1). Incubation with the same volume of DMSO was used as control. The next day, cell extract and supernatant were collected, separated by non-denaturing PAGE and analyzed by Western Blot (Figure 3.12 to Figure 3.15). Afterwards, membranes were cut above the 146 kDa marker band to allow simultaneous investigation of NS polymers and PDI, the loading control. Every treatment was performed in three technical replicates and every experiment has been carried out two times.

NS^{G392E} polymers appear in cell extract and supernatant. Their molecular weight is above 242 kDa. The bands corresponding to the PDI signal are at approximately 66 kDa.

Intensities of the smeared bands representing NS polymers in cell extract and supernatant were measured and normalized to the corresponding PDI signal. The means and standard deviations of six measurements per compound are plotted in Figure 3.16 and set relative to the DMSO control. A two-sided student's t-test was used to calculate p-values and identify compounds that inhibit polymerization significantly (Table 3.5).

Significant reduction of NS polymers can be observed in supernatant after treatment with compounds G (0.72 ± 0.10 , $p = 0.0032$), O (0.71 ± 0.09 , $p = 0.0002$) and R (0.77 ± 0.13 , $p = 0.0312$). Compound N leads to a significant reduction of polymers in cell extract (0.88 ± 0.10 , $p = 0.0429$). No other compound lowers the amount of NS polymers in cell extract significantly. However, treatment with five different compounds cause a significant increase of polymers within the cell: A (1.71 ± 0.33 , $p = 0.0019$), B (1.21 ± 0.09 , $p = 0.0167$), G (2.24 ± 0.69 , $p = 0.0068$), J (1.47 ± 0.22 , $p = 0.0018$) and Q (1.59 ± 0.39 , $p = 0.0131$).

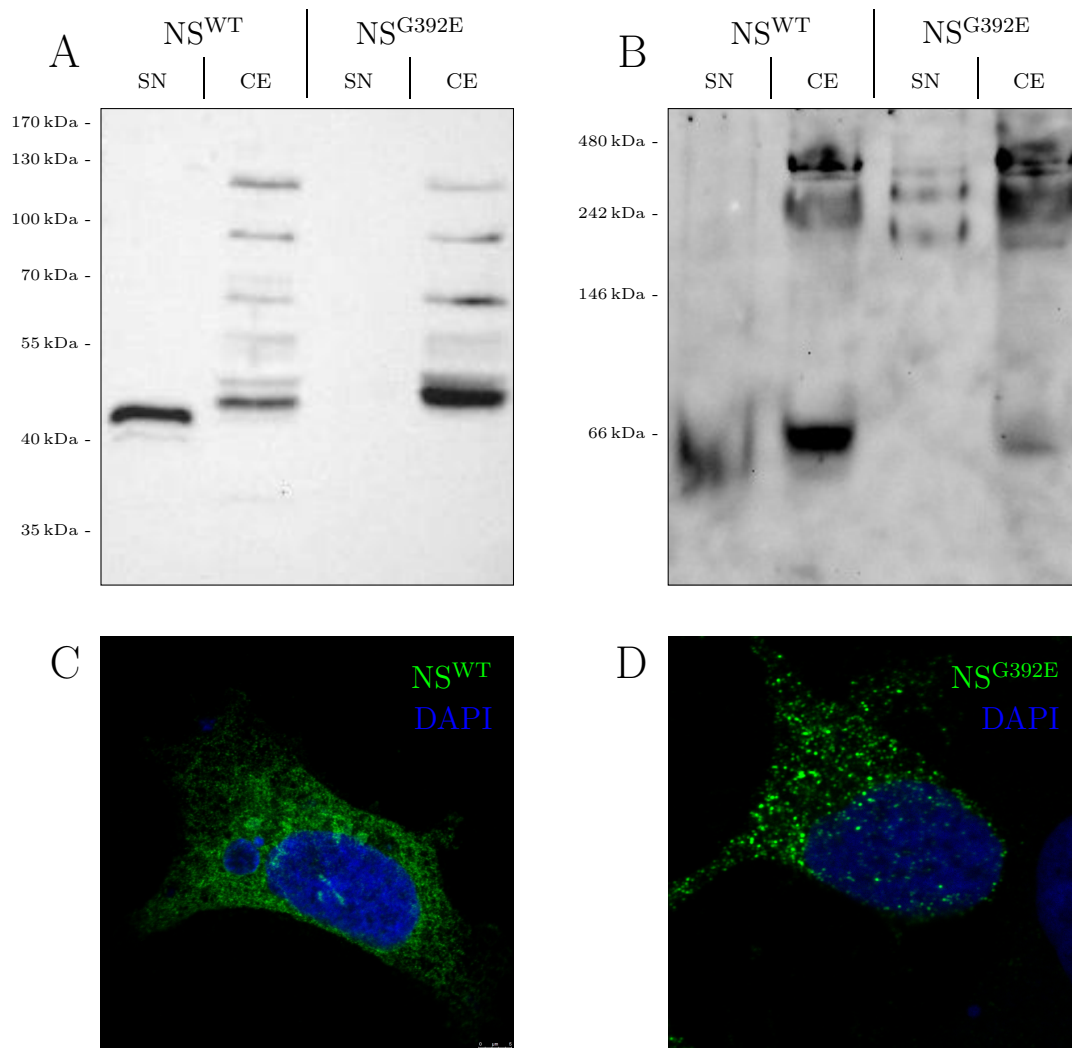


Figure 3.10: Characterization of stably transfected HEK-293-cells overexpressing either NS^{WT} or NS^{G392E}. (A) and (B) show Western Blots of supernatant (SN) and cell extract (CE) after SDS-PAGE and non-denaturing PAGE, respectively. Both membranes were stained with an antibody directed against NS. (C) and (D) show representative immunocytochemical stainings of HEK-293-cells overexpressing NS^{WT} and NS^{G392E}, respectively. NS is shown in green.

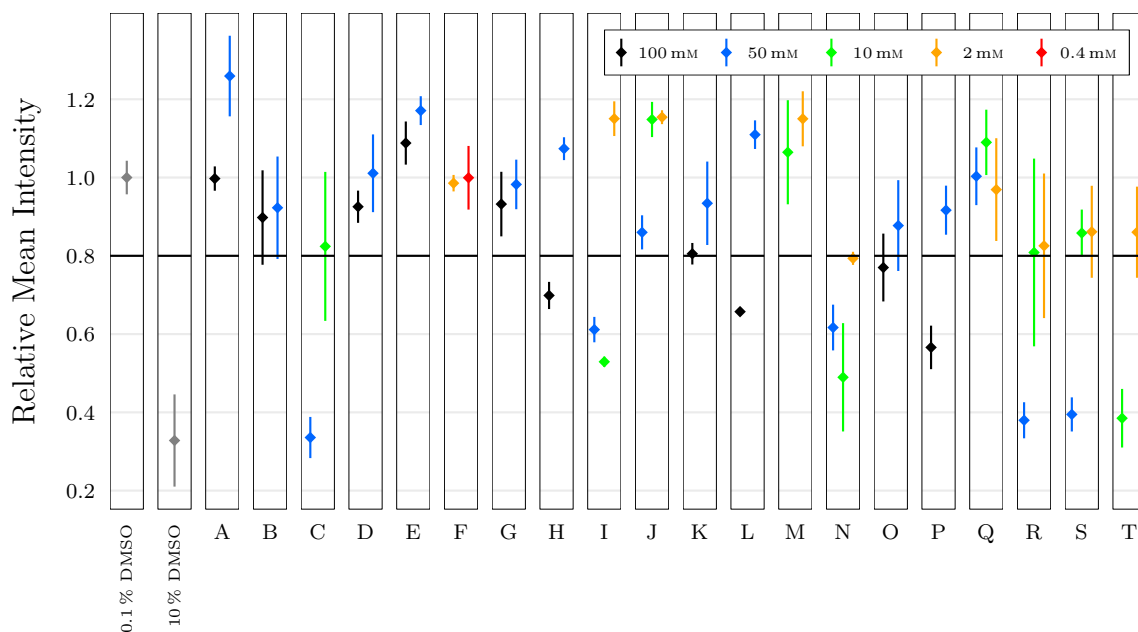


Figure 3.11: MTT cell proliferation assay to determine a suitable concentration of 1st generation compounds for *in vivo* experiments. Stably transfected NSG^{392E}-cells were incubated overnight with 1st generation compounds at concentrations varying from 0.4 μM to 100 μM . As a positive and negative control for cell proliferation, cells were incubated with a medium containing 0.1% DMSO and 10% DMSO, respectively. Cell proliferation was measured using the CellTiter 96[®] Non-Radioactive Proliferation Assay. Measured absorptions were normalized to the positive DMSO control (0.1%). Means and standard deviations are plotted ($n = 4$). The highest concentration allowing 80% (0.8 value) compared to the 0.1% DMSO control was chosen for further experiments.

Table 3.5: *In vivo* screening experiment with 1st generation compounds

	cell extract			supernatant		
	rel. mean	SD±	p-value	rel. mean	SD±	p-value
DMSO	1.00	0.14		1.00	0.15	
A	1.71	0.33	0.0019	1.11	0.27	0.4005
B	1.21	0.09	0.0167	1.20	0.20	0.0780
C	1.06	0.28	0.6525	0.93	0.33	0.6461
D	0.90	0.10	0.3402	0.86	0.36	0.4354
E	1.15	0.08	0.1454	1.10	0.46	0.6397
F	1.08	0.20	0.5064	1.23	0.40	0.2672
G	2.24	0.69	0.0068	0.72	0.10	0.0032
H	1.01	0.07	0.9066	0.98	0.13	0.7951
I	0.99	0.14	0.8937	1.07	0.13	0.4129
J	1.47	0.22	0.0018	0.87	0.13	0.1293
K	0.82	0.16	0.0568	1.08	0.15	0.3342
L	1.34	0.37	0.0731	1.02	0.35	0.8841
M	1.09	0.16	0.2234	0.91	0.10	0.1082
N	0.88	0.10	0.0429	0.86	0.16	0.1123
O	1.14	0.15	0.0740	0.71	0.09	0.0002
P	0.98	0.30	0.8609	1.06	0.37	0.7311
Q	1.59	0.39	0.0131	0.84	0.36	0.3750
R	1.23	0.29	0.1277	0.77	0.13	0.0312
S	1.15	0.21	0.2266	1.21	0.35	0.2068
T	0.82	0.24	0.1906	0.75	0.28	0.0944

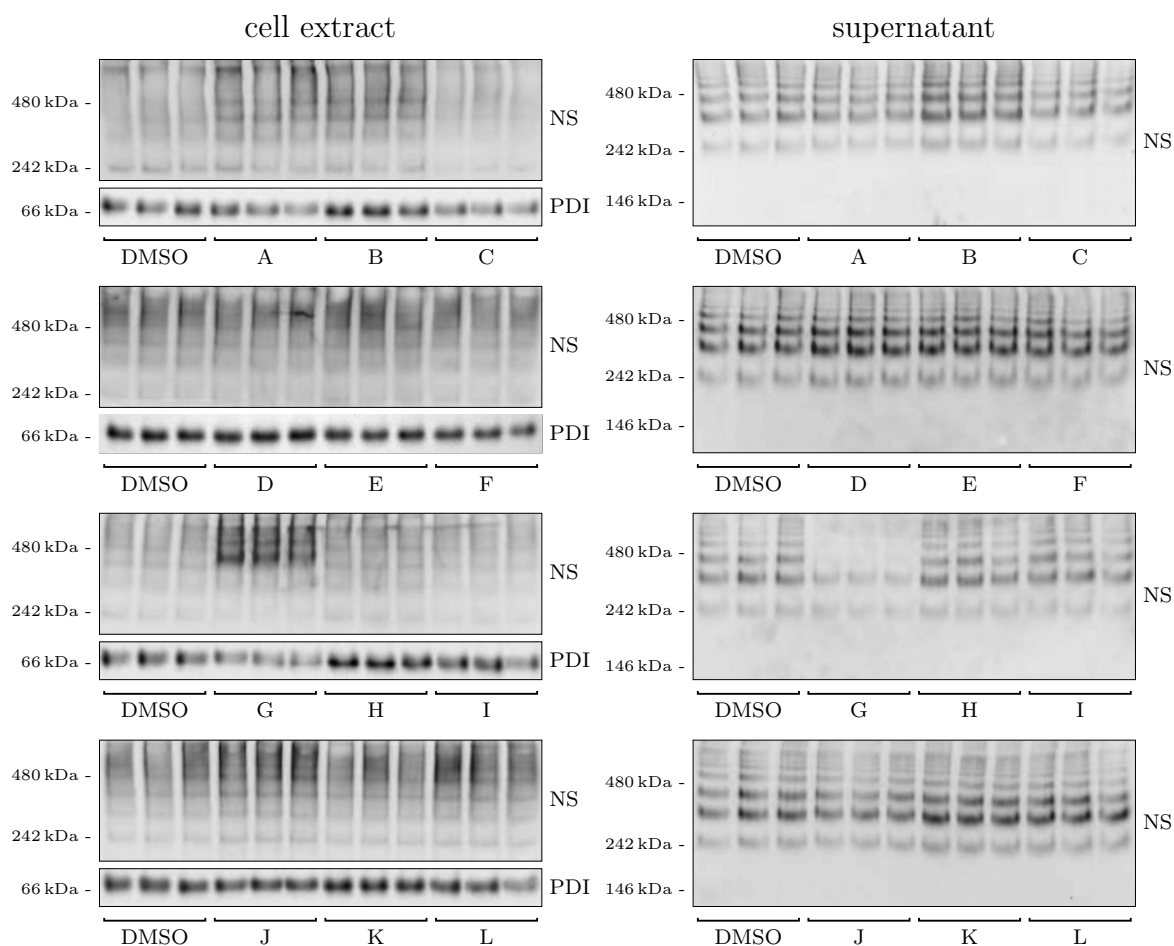


Figure 3.12: *In vivo* screening assay with 1st generation compounds (triplicate set 1 of 2, compounds A-L). Stably transfected NS^{G392E}-cells were treated overnight with a compound. DMSO served as a control. The next day supernatant and cell extract were collected and analyzed by non-denaturing PAGE and Western Blot. Membranes were probed with antibodies against NS and PDI (as housekeeping protein). Each experiment was performed in triplicate. NS polymer formation was evaluated in cell extract and supernatant separately.

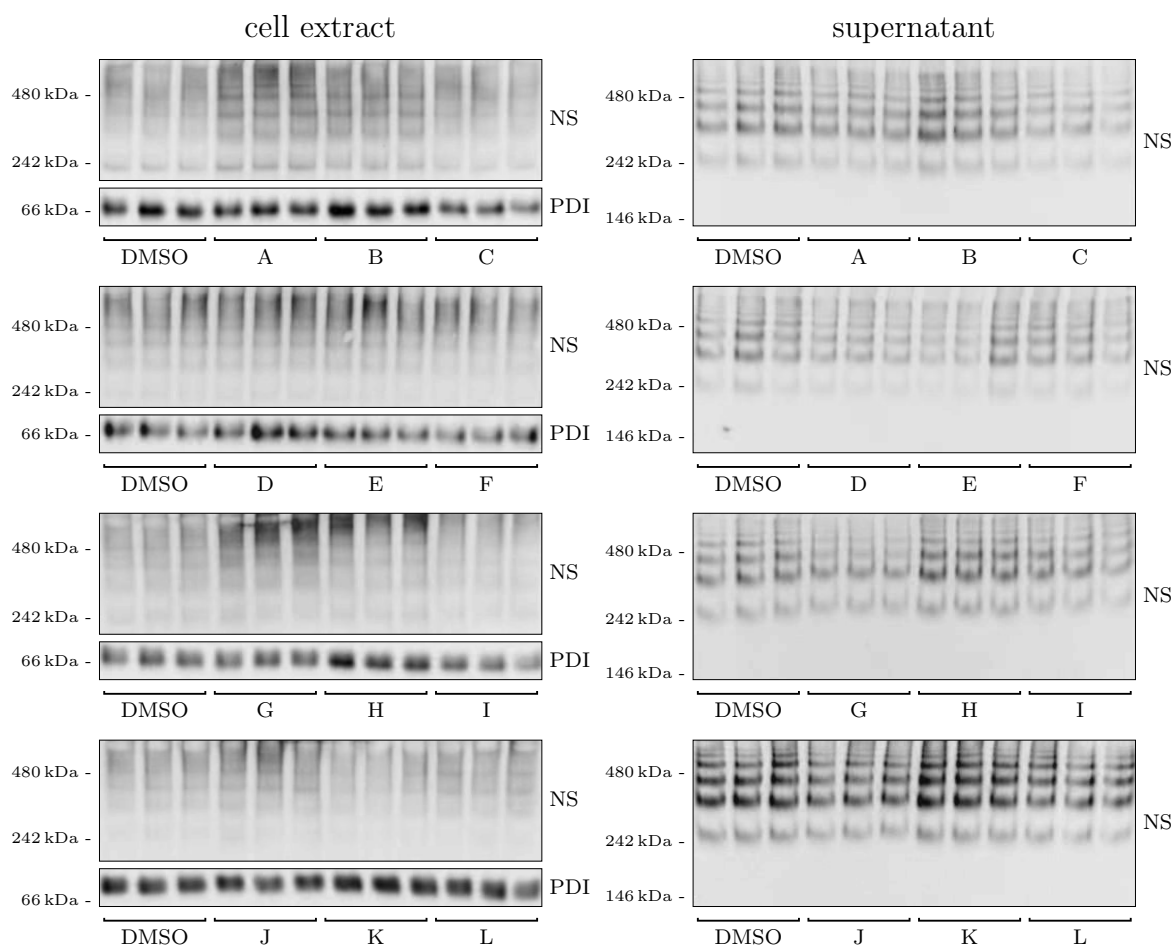


Figure 3.13: *In vivo* screening assay with 1st generation compounds (triplicate set 2 of 2, compounds A-L). Stably transfected NS^{G392E}-cells were treated overnight with a compound. DMSO served as a control. The next day supernatant and cell extract were collected and analyzed by non-denaturing PAGE and Western Blot. Membranes were probed with antibodies against NS and PDI (as housekeeping protein). Each experiment was performed in triplicate. NS polymer formation was evaluated in cell extract and supernatant separately.

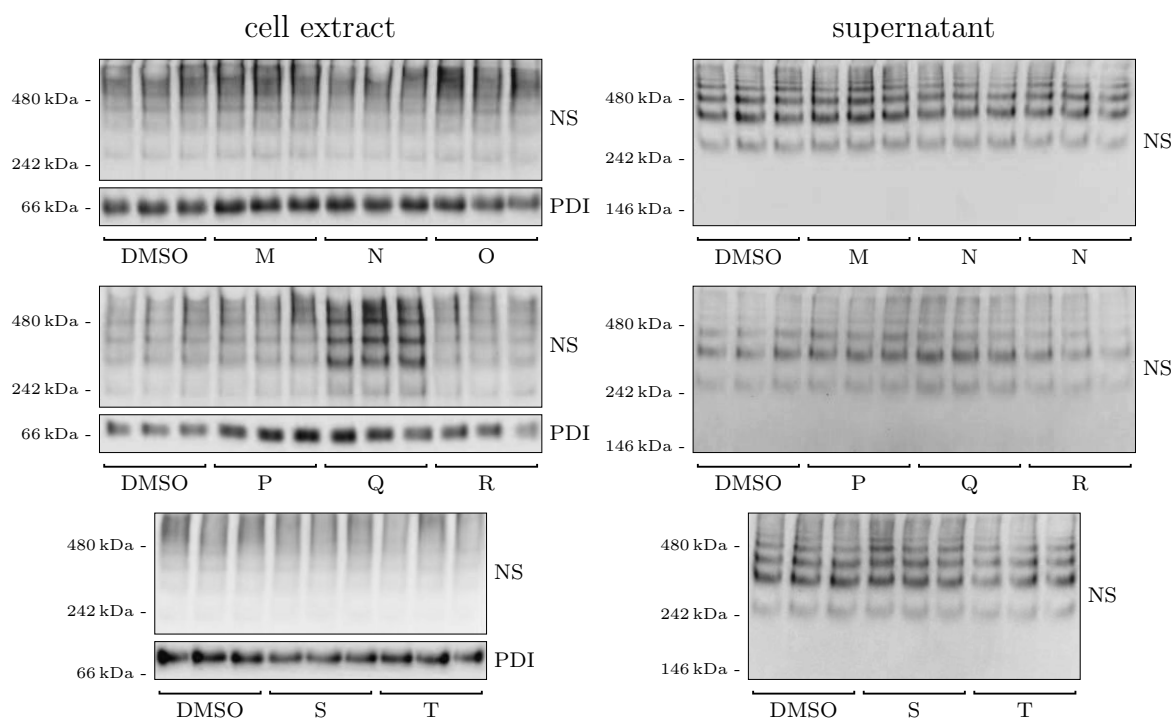


Figure 3.14: *In vivo* screening assay with 1st generation compounds (triplicate set 1 of 2, compounds M-T). Stably transfected NS^{G392E}-cells were treated overnight with a compound. DMSO served as a control. The next day supernatant and cell extract were collected and analyzed by non-denaturing PAGE and Western Blot. Membranes were probed with antibodies against NS and PDI (as housekeeping protein). Each experiment was performed in triplicate. NS polymer formation was evaluated in cell extract and supernatant separately.

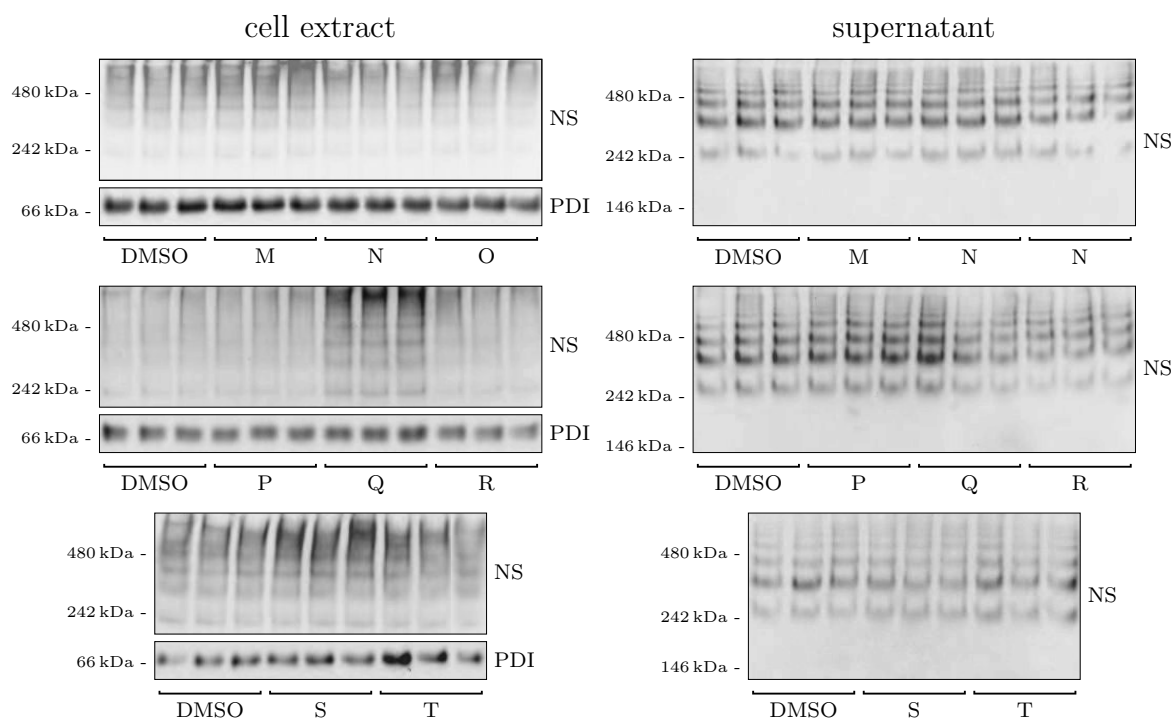


Figure 3.15: *In vivo* screening assay with 1st generation compounds (triplicate set 2 of 2, compounds M-T). Stably transfected NS^{G392E}-cells were treated overnight with a compound. DMSO served as a control. The next day supernatant and cell extract were collected and analyzed by non-denaturing PAGE and Western Blot. Membranes were probed with antibodies against NS and PDI (as housekeeping protein). Each experiment was performed in triplicate. NS polymer formation was evaluated in cell extract and supernatant separately.

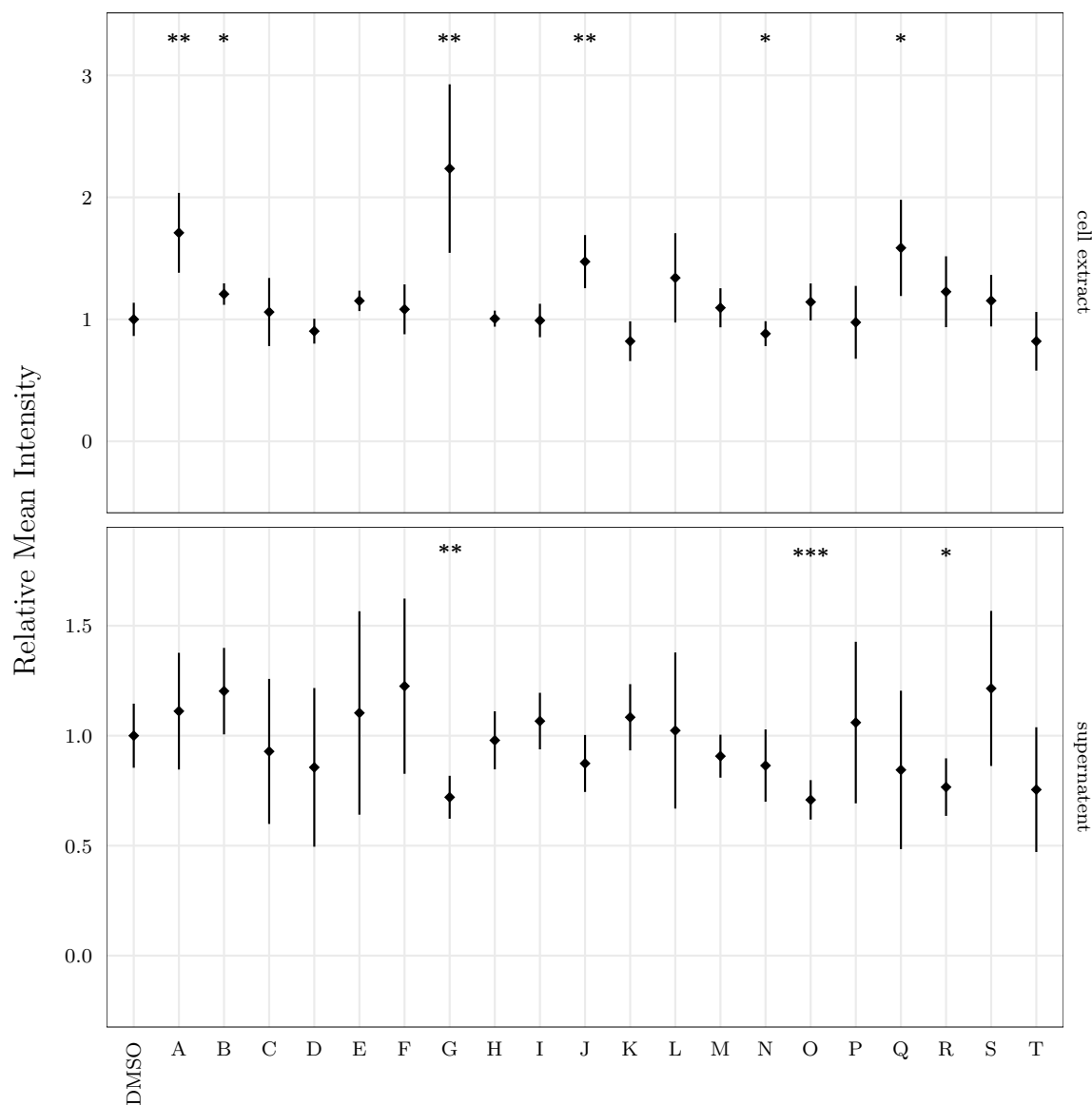


Figure 3.16: Quantification of *in vivo* screening experiment with 1st generation compounds. Band intensities of the polymer ladders in cell extract (upper box) and supernatant (lower box) were normalized to the corresponding PDI-intensity. The data of two independent sets of triplicates was averaged and the DMSO control was set to 1 (see figures 3.12 to 3.15, $n = 6$). Asterisks indicate a significant difference to the DMSO control ($* \hat{=} p\text{-value} < 0.05$, $** \hat{=} p\text{-value} < 0.01$, $*** \hat{=} p\text{-value} < 0.001$, students t-Test).

4 Discussion

Dementia is the leading cause of dependency, disability and institutionalization among older populations (Sindi et al., 2015). Due to an expected increase in life expectancy over the next decades, the prevalence rates of dementia syndromes are thought to rise significantly (Prince et al., 2013). Clinicians and health care specialists are therefore faced with the increasing challenge to find reasonable treatment options. In order to discover specific treatments an exact understanding of the underlining disease is of the essence.

A common element of various dementia types is the aggregation of misfolded proteins (Crowther, 2002). With increasing age the cellular mechanisms responsible for clearance of toxic aggregates decline leading to neuronal death and appearance of first symptoms (Schipanski et al., 2013).

Understanding the mechanism of protein aggregation opens the possibility to design disease specific drugs. By preventing aggregation, these drugs would assist the cellular degradation apparatus and thus prolong the course of disease (Lomas and Carrell, 2002).

FENIB is an inheritable dementia that is caused by the intracellular accumulation of polymeric NS into so called Collins bodies. Patients carrying mutations that cause FENIB suffer from inexorable deterioration of cognitive functions leading to early onset dementia often accompanied by difficult-to-treat epilepsy (Davis et al., 1999b).

NS belongs to the well studied protein superfamily of serine protease inhibitors (serpins) (Davis et al., 1999b). Throughout the serpin family, mutations that cause the polymerization of serpins can be found. These genetic diseases are called serpinopathies (Lomas and Carrell, 2002).

Finding a treatment solution for serpinopathies like FENIB will not only be directly beneficial for patients affected by the particular disease. Because of the overlap of disease mechanisms, the gathered knowledge can be applied to other serpinopathies as well (Lomas and Carrell, 2002).

Here we screened 36 small chemical compounds obtained from two rounds of virtual ligand screening using an *in silico* model of RCL insertion.

Because of their small size, these compounds are likely to cross the BBB and traverse the cell membrane to reach the ER. We hypothesized that they inhibit polymerization by inserting into β -sheet A and blocking the loop-sheet-linkage of

NS^{G392E}, one of the most destructive mutations known.

For this study, we developed two screening methods to test the compound's anti-polymerizing activity. Recombinant NS^{WT} and NS^{G392E} protein was utilized in an *in vitro* experiment. Additionally, 1st generation compounds were tested in an *in vivo* assay using stably transfected HEK-293-cells overexpressing NS^{G392E}.

4.1 Compound BUR reduces polymerization of recombinant NS^{WT}

Recombinantly produced serpins like α -1-antitrypsin or NS have been used previously to test substances for their anti-polymerization activity. The heating for a certain time results in the polymerization even of wild type serpins (Chang et al., 2006, 2009, Elliott et al., 2000, Mahadeva et al., 2002, Mallya et al., 2007, Saga et al., 2016).

When separated by native PAGE, recombinant NS^{WT} is mainly found in its monomeric form (see lane 1 of upper row gels in Figure 3.1 to Figure 3.7). Heating at 37 °C for 16 hours results in the formation of polymers (see lane 2).

Adding compound BUR to recombinant NS^{WT} leads to significantly less polymers after treatment (from 54% [\pm 7%] to 39% [\pm 5%], $p = 0.0032$). Furthermore, the amount of dimers is significantly increased to a level comparable to the unheated control (from 22% [\pm 4%] to 32% [\pm 6%], $p = 0.0358$, unheated control: 31% [\pm 5%]). Although not statistically significant, a tendency towards a rescue of the monomeric state can also be observed (from 24% [\pm 5%] to 29% [\pm 5%], $p = 0.1037$) (Figure 3.4 to Figure 3.7 and Figure 3.9, Table 3.3).

This *in vitro* behaviour suggests that BUR prevents the RCL-insertion of a next molecule and therefore polymer formation probably by binding to β -sheet A of recombinant NS^{WT}.

However, the measured effect is only moderate. Untreated NS^{WT} consists of 17% (\pm 8%) polymers. After incubation at 37 °C, the polymer count rises to 54% (\pm 7%) — an approximate 3-fold increase. The presence of compound BUR in the solution inhibits polymer formation to a total of 39% (\pm 5%) polymers which is still a 2-fold increase compared to unheated control (Table 3.3 and Figure 3.9).

This moderate effect size could be due to an insufficient binding affinity towards β -sheet A. Small changes within the molecular structure of BUR might improve the binding. Future research will show if compounds derived from BUR have a greater impact on inhibiting polymerization.

Moreover, further *in vivo* testing will clarify if BUR can be used as an anti-polymerization-agent in a cell model and thereafter possibly in an animal model of

FENIB.

Unfortunately, the remaining tested compounds showed no anti-polymerization-effect on recombinant NS^{WT} *in vitro*. Again, the reason may be poor binding affinity to β -sheet A.

4.2 Recombinant NS^{G392E} consists primarily of polymers prior to incubation

The *in vitro* assay was extended by the analysis of recombinant NS^{G392E}.

However, even untreated NS^{G392E} appears to be polymerized prior to incubation at 37 °C for 16 hours. After incubation, no significant difference is detectable (Figure 3.8 and Figure 3.9, Table 3.2 and Table 3.4). This could be due to polymer formation directly after its recombinant production.

This is not surprising since the NS^{G392E} mutation causes one of the most severe disruption to the conformational stability of NS. Glycine 392 is necessary for the correct alignment of adjacent phenylalanines and is essential for the stabilization of the shutter region. The replacement by glutamate (NS^{G392E}) or arginine (NS^{G392R}) results in the most severe forms of FENIB known today (Davis et al., 2002).

Since recombinant NS^{G392E} could not be used to investigate polymer formation, we tested if incubation with compounds could efficiently dissolve pre-formed polymers of NS^{G392E}. This is an important issue, as serpinopathies are often diagnosed when a substantial amount of polymers have already been formed.

Unfortunately, no compound proved to be able to reverse polymerization (Figure 3.1 to Figure 3.7 and Figure 3.8 to Figure 3.9). However, a slight increase in polymers was detected after treatment with compound O (from 70% [$\pm 4\%$] to 78% [$\pm 3\%$], $p = 0.0450$). Not only is this result contrary to the objective of this study, the measured effect is also rather small.

It remains unclear whether compound BUR would inhibit polymerization when added to a solution of monomeric NS^{G392E}. To be able to test this, the production of recombinant protein has to be altered to reduce polymerization prior to the experiment. A possible solution could be the production of recombinant NS^{G392E} at very low temperatures.

Another approach would be to directly test the compound in an *in vivo* environment. The presence of a promising compound like BUR during NS protein synthesis might result in the blockage of β -sheet A prior to RCL insertion.

4.3 NS^{G392E} cells are a suitable cell culture model of FENIB

A variety of different animal and cell culture models have been used as models of FENIB before (Galliciotti et al., 2007, Guadagno et al., 2017, Miranda et al., 2008, Saga et al., 2016, Schipanski et al., 2014).

In the present work, 1st generation compounds were screened using a HEK-293 cell model stably overexpressing NS^{G392E}. HEK-293-cells have been used extensively for decades and proved to be an easy to handle and manipulate cell culture (Graham et al., 1977, Schipanski et al., 2014). Before starting the compound screening, we characterized expression and localization of both NS^{WT} and NS^{G392E} in the HEK-293-cells.

Previous work has shown that NS^{WT} is post-translationally processed within the ER and then secreted through vesicles via the Golgi apparatus (Ishigami et al., 2007). Mutant NS, however, forms polymers that are retained within the ER and eventually form large aggregates called Collins bodies (Davis et al., 1999b).

Our cell model nicely reflects this predicted subcellular behaviour. This can be demonstrated by analyzing HEK-293-cells overexpressing either NS^{WT} or NS^{G392E} with denaturing SDS and native PAGE (Figure 3.10, A and B).

In SDS-PAGE, NS^{WT} can be found in both cell extract and supernatant as a single band of approximately 45 kDa, suggesting that NS^{WT} is synthesized and secreted as expected (Figure 3.10, A and B). Bands of weak intensity above 50 kDa both in NS^{WT} and NS^{G392E} cell extracts are most likely unspecific background noise by the antibody (Figure 3.10, A).

Similarly, native PAGE confirms the presence of NS^{WT} in its monomeric form in both cell extract and supernatant (Figure 3.10, B).

Contrary to NS^{WT}, NS^{G392E} is known to rapidly form polymers within the ER that are mostly retained there. When analysed with denaturing SDS-PAGE, this shows as a single band only in cell extract (Figure 3.10, A). Western Blotting after native PAGE reveals polymeric NS^{G392E} to be separated into a high molecular weight ladder (Figure 3.10, B). Only a faint band representing NS^{G392E} in monomeric form was observed.

Interestingly, a faint polymer ladder can be found not only in cell extract but also in supernatant (lane 3, Figure 3.10, B). This could be in part explained by an increase in cell death and subsequent contamination of the supernatant with intracellular molecules. However, no increased cell death was observed when handling the cell cultures. Moreover, secreted polymers have been previously found in the media of different cell culture models of FENIB (Guadagno et al., 2017, Miranda et al., 2004,

2008). Guadagno et al. (2017) cultivated neural progenitor cells derived from mouse cerebral cortex. Native PAGE and Western Blotting show similar polymer ladders in the media of this neuronal cell culture. This suggests a previously unexamined mechanism of partial NS polymer secretion.

More evidence that NS^{G392E} cells represent a suitable model for screening assays comes from immunocytochemistry experiments. In NS^{WT} cells the immunofluorescence signal is evenly distributed in an ER-cisternae-like pattern as previously described (Figure 3.10, C) (Oberhauser, 2013, Schipanski et al., 2014). As expected, NS^{G392E} accumulates as numerous dots within the cell bodies indicating polymer formation (Figure 3.10, D).

Taken together, our results show that HEK-293-cells overexpressing NS^{G392E} represent a valid cell culture model for FENIB.

4.4 Compound G enhances polymer retention in vivo

Twenty 1st generation compounds were screened for their ability to inhibit polymerization of NS^{G392E} in the HEK-293-cells model, eight compounds altered the amount of polymers significantly.

When examining intracellular polymers in cell extract, only compound N had a polymer reducing effect. While being statistically significant, the measured effect is considerably small with a reduction to only 88% ($\pm 10\%$, $p = 0.0429$) compared to control ($100\% \pm 14\%$). Moreover, the polymer reduction in supernatant was not significant. In the *in vitro* experiment compound N had no significant effect on the polymerization of recombinant NS^{WT} or NS^{G392E}.

Five compounds had an opposing, polymer increasing effect in cell extract: A (171% [$\pm 33\%$], $p = 0.0019$), B (121% [$\pm 9\%$], $p = 0.0167$), G (224% [$\pm 69\%$], $p = 0.0068$), J (147% [$\pm 22\%$], $p = 0.0018$) and Q (159% [$\pm 39\%$], $p = 0.0131$).

While this is seemingly an unfavorable effect, it is particularly interesting in the case of compound G. Treatment with compound G not only increased the amount of polymers within the cell more than two-fold, but it also reduced the extracellular amount of NS^{G392E} polymers to 72% ($\pm 10\%$, $p = 0.0032$). Compounds A, B, J and Q had no polymer altering activity in supernatant.

These findings give rise to three alternative conclusions for the intriguing *in vivo* behavior of compound G.

One possible explanation is that the presence of compound G leads to increased interaction between mutant NS and cell membrane. During protein extraction, polymers that were originally secreted into supernatant would wrongly be detected in cell extract.

Another conceivable explanation is that compound G interferes with NS in a way that rather enhances the polymerization rate within the cell. Compound G might bind to β -sheet A but instead of blocking the RCL from insertion it might destabilize the sheet further and thus even promote loop linkage. The enhanced polymerization of NS might in turn result in an increased retention within the cell and reduced secretion into media. *In vitro* we did not detect any increase in polymer formation in the presence of compound G. The opposing results obtained from the *in vivo* and *in vitro* assay might be explained by slight changes in the structure of recombinant NS produced in E.coli compared to NS synthesized by HEK-293-cells (e.g. glycosylation state, unphysiological conditions).

Another possibility why compound G seems to have no impact on recombinant NS might be due to the limitations of the *in vitro* assay. Compound G might only have an effect on NS^{G392E} and not NS^{WT}. This might be masked by the fact that NS^{G392E} is already polymerized prior to the treatment with compounds. Such an effect might only be detectable in the *in vivo* experiment since compound G would be present during biosynthesis and prior to polymerization.

The combination of these considerations leads to the third explanation for the unique *in vivo* polymerization pattern: Compound G might not interact with NS at all. Instead, a role as an inhibitor of pathways involved in the secretion of polymeric NS seems plausible. To our best knowledge, such pathways have not yet been investigated. However, the data from different cell culture models, including ours, strongly suggest that mechanisms exist to secrete polymeric NS into media (Guadagno et al., 2017, Miranda et al., 2004, 2008). Inhibition of such pathways would result in the observed retention of NS^{G392E} in cell extract and lower amount of secreted polymers.

Interestingly, the effects of compound G on NS^{G392E} cells do not result in increased cell death due to protein overload. Even a treatment at a concentration as high as 100 mM results in no significant change of cell proliferation (Figure 3.11). This leads to the conclusion that increased intracellular polymers are not particularly toxic to HEK-293-cells. In fact, this has been reported for a number of cell culture models of FENIB including COS-7 cells (Miranda et al., 2004), PC12 cells (Miranda et al., 2008) and HeLa cells (Roussel et al., 2013). While this might be due to the strong proliferative nature of these cultures, a recent study comes to similar conclusions for a neural progenitor cell model derived from mouse cerebral cortex (Guadagno et al., 2017).

If intracellular polymer accumulation in itself is not harmful, then secreted extracellular NS polymers might be toxic to neurons and eventually cause neurodegeneration in FENIB. Further work is now needed to investigate this possibility. In case extracellular mutant NS plays a role in the pathogenesis of FENIB, the treatment

with compound G inhibiting polymer accumulation in the extracellular space might be promising.

Additionally to compound G, the treatment with two other compounds led to a significant reduction of polymers in the supernatant: O (71% [$\pm 9\%$], $p = 0.0002$) and R (77% [$\pm 13\%$], $p = 0.0312$). Again, this anti-polymerizing effect was not detectable in the *in vitro* assay. In principle, the same assumption apply for these two compounds as for compound G. However, in contrast to compound G, these compounds had no effect on polymers in cell extract, suggesting that they may not reach the intracellular space.

4.5 Conclusions

Aim of this study was the screening of small chemical compounds that efficiently prevent loop-sheet-polymerization by binding to β -sheet A of mutant NS. For this purpose, we successfully develop two assays: the *in vitro* assay utilizes recombinant NS^{WT} and NS^{G392E} produced in E.coli and allows to rapidly test many compounds simultaneously. In the *in vivo* assay, in addition to the anti-polymerization activity of the compounds, their toxicity and ability to penetrate the cell were investigated using a HEK-293-cells model.

Compound BUR successfully reduced polymer formation in the *in vitro* assay. However, compound BUR was not able to dissolve already formed NS polymers. Further research is needed to show if slight alteration to the structure of compound BUR will create compounds with higher anti-polymerizing activity.

Twenty of the 36 compounds were further tested in the *in vivo* cell model of FENIB. The most interesting result was obtained with compound G that significantly reduced the amount of mutant NS secreted by the cells. However, an increased accumulation of polymers within the cell became apparent. Since compound G had no effect on polymerization of recombinant NS^{WT} or NS^{G392E} *in vitro*, we speculate that it may rather affect pathways involved in the secretion of NS polymers. Further work is needed to identify such pathways and to understand the pathological role of secreted NS polymers. The unique effect of compound G might prove useful to antagonize possible extracellular toxic events.

Abstract

FENIB is an autosomal dominantly inherited neurodegenerative disease that leads to early onset dementia and epilepsy. It is caused by point mutations in NS, a serine protease inhibitor (serpin) predominantly expressed in the nervous system. These mutations lead to polymerization and accumulation of pathological mutants in cortical inclusion bodies. Polymer formation is caused by sequential insertion of the reactive center loop of one NS mutant into the β -sheet A of another.

Using molecular dynamics simulations, small chemical compounds with high binding affinities to β -sheet A were identified as potential candidates to block loop-sheet-insertion. Here, we developed a screening assay to test 36 of these pre-selected compounds utilizing recombinantly produced NS. Additional to this *in vitro* characterization, 20 compounds were further tested in a cell culture model of FENIB.

We found that one compound (BUR) successfully reduced polymer formation in the *in vitro* assay. However, already formed polymers were not dissolved. Further research is needed to show if structural alterations to compound BUR enhance the anti-polymerizing effect.

Another compound (G) significantly reduced the amount of NS polymers secreted by cells. However, intracellularly, increased amounts of polymerized NS were measured. Additionally, compound G showed no effect on recombinant NS in the *in vitro* experiments. Rather than inhibiting polymerization, we speculate that compound G might interact with pathways involved in secretion of mutant NS. Investigation of such pathways will possibly shed light on mechanisms of mutant NS toxicity.

Zusammenfassung

FENIB ist eine autosomal dominant vererbte neurodegenerative Erkrankung, welche zu einer frühen Form der Demenz und Epilepsie führt. Sie wird durch Punktmutationen im Neuroserpin-Gen verursacht, ein Serin-Protease-Inhibitor, der hauptsächlich im zentralen Nervensystem exprimiert wird. Diese Mutationen führen zu einer vermehrten Polymerisation und Akkumulation von pathologischen Neuroserpin-Mutanten in kortikalen Einschlusskörperchen. Zur Polymer-Bildung kommt es durch die aufeinanderfolgende Insertion der reaktiven Zentralschleife eines Neuroserpin-Moleküls in das β -Faltblatt A eines anderen.

In dieser Arbeit entwickelten wir ein Screening-Verfahren, um 36 chemische Verbindungen auf ihre Fähigkeit hin zu testen, die Insertion der Zentralschleife zu verhindern. Diese Verbindungen haben in einer vorangegangenen Molekulardynamik-Simulation eine hohe Bindungsaffinität zum β -Faltblatt A gezeigt und könnten sich daher durch eine Blockade der Insertion als therapeutische Option eignen. Für dieses Screening-Analyse wurde rekombinant hergestelltes Neuroserpin verwendet. Zusätzlich zu dieser *in vitro* Untersuchung wurden 20 dieser Substanzen in einem FENIB-Zellmodell getestet.

In der *in vitro* Analyse konnte gezeigt werden, dass eine der untersuchten Verbindungen (BUR) die Polymer-Bildung erfolgreich reduzieren konnte. Bedauerlicherweise konnten bereits geformte Polymere durch diese Verbindung nicht aufgelöst werden. Weitere Untersuchungen sind notwendig, um zu zeigen, ob Veränderungen an der Molekülstruktur von BUR zu einer Verbesserung des Anti-Polymerisation-Effektes führen.

Im Zellmodell zeigte eine weitere Verbindung (G) eine signifikante Reduzierung der Neuroserpin-Sekretion. Gleichzeitig wurde intrazellulär eine erhöhte Neuroserpin-Konzentration gemessen. Da die Verbindung G keinen Effekt auf rekombinantes Neuroserpin zeigte, vermuten wir, dass diese Resultate im Sinne einer Interaktion im Sekretionsweg von mutiertem Neuroserpin zu deuten sind. Weiterführende Untersuchungen solcher Sekretionswege könnten Aufschluss geben über die Mechanismen der Toxizität von Neuroserpin-Mutanten in FENIB.

Bibliography

- H. Amano-Takeshige, G. Oyama, K. Kanai, T. Miyagawa, J. Mitsui, Y. Ugawa, S. Tsuji, and N. Hattori. A Japanese family with mutation in the proteinase inhibitor 12 L47P gene: A case report. *Journal of the Neurological Sciences*, 384: 126–128, 2018.
- A. Baron, A. Montagne, F. Cassé, S. Launay, E. Maubert, C. Ali, and D. Vivien. NR2D-containing NMDA receptors mediate tissue plasminogen activator-promoted neuronal excitotoxicity. *Cell Death and Differentiation*, 17(5):860–871, 2010.
- D. Belorgey, D. C. Crowther, R. Mahadeva, and D. A. Lomas. Mutant Neuroserpin (S49P) that causes familial encephalopathy with neuroserpin inclusion bodies is a poor proteinase inhibitor and readily forms polymers in vitro. *J Biol Chem*, 277(19):17367–17373, 2002.
- D. Belorgey, L. K. Sharp, D. C. Crowther, M. Onda, J. Johansson, and D. A. Lomas. Neuroserpin Portland (Ser52Arg) is trapped as an inactive intermediate that rapidly forms polymers: Implications for the epilepsy seen in the dementia FENIB. *Eur J Biochem*, 271(16):3360–3367, 2004.
- D. Belorgey, P. Hägglöf, S. Karlsson-Li, and D. A. Lomas. Protein misfolding and the serpinopathies. *Prion*, 1(1):15–20, 2007.
- M. Bergener and L. Gerhard. [Myoclonic bodies and progressive myoclonic epilepsy]. *Der Nervenarzt*, 41(4):166–173, 1970.
- S. F. Berkovic, F. Andermann, S. Carpenter, and L. S. Wolfe. Progressive myoclonus epilepsies: Specific causes and diagnosis. *The New England Journal of Medicine*, 315(5):296–305, 1986a.
- S. F. Berkovic, S. Carpenter, and F. Andermann. Atypical inclusion body progressive myoclonus epilepsy: A fifth case? *Neurology*, 36(9):1275–1276, 1986b.
- V. M. Borges, T. W. Lee, D. L. Christie, and N. P. Birch. Neuroserpin regulates the density of dendritic protrusions and dendritic spine shape in cultured hippocampal neurons. *Journal of Neuroscience Research*, 88(12):2610–2617, 2010.

- C. B. Bradshaw, R. L. Davis, A. E. Shrimpton, P. D. Holohan, C. B. Rea, D. Fieglin, P. Kent, and G. H. Collins. Cognitive Deficits Associated With a Recently Reported Familial Neurodegenerative Disease: Familial Encephalopathy With Neuroserpin Inclusion Bodies. *Arch Neurol*, 58(9):1429–1434, 2001.
- Y.-P. Chang, R. Mahadeva, W.-S. W. Chang, A. Shukla, T. R. Dafforn, and Y.-H. Chu. Identification of a 4-mer peptide inhibitor that effectively blocks the polymerization of pathogenic Z alpha1-antitrypsin. *American Journal of Respiratory Cell and Molecular Biology*, 35(5):540–548, 2006.
- Y.-P. Chang, R. Mahadeva, W.-S. W. Chang, S.-C. Lin, and Y.-H. Chu. Small-molecule peptides inhibit Z alpha1-antitrypsin polymerization. *J Cell Mol Med*, 13(8B):2304–2316, 2009.
- A. Chevilley, F. Lesept, S. Lenoir, C. Ali, J. Parcq, and D. Vivien. Impacts of tissue-type plasminogen activator (tPA) on neuronal survival. *Frontiers in Cellular Neuroscience*, 9, 2015.
- P. Cinelli, R. Madani, N. Tsuzuki, P. Vallet, M. Arras, C. N. Zhao, T. Osterwalder, T. Rüllicke, and P. Sonderegger. Neuroserpin, a neuroprotective factor in focal ischemic stroke. *Mol Cell Neurosci*, 18(5):443–457, 2001.
- J. W. Cole, A. C. Naj, J. R. O’Connell, O. C. Stine, J. D. Sorokin, M. A. Wozniak, B. J. Stern, M. Yepes, D. A. Lawrence, L. J. Reinhart, D. K. Strickland, B. D. Mitchell, and S. J. Kittner. Neuroserpin polymorphisms and stroke risk in a biracial population: The stroke prevention in young women study. *BMC Neurol*, 7:37, 2007.
- L. Cong, F. A. Ran, D. Cox, S. Lin, R. Barretto, N. Habib, P. D. Hsu, X. Wu, W. Jiang, L. Marraffini, and F. Zhang. Multiplex Genome Engineering Using CRISPR/Cas Systems. *Science*, page 1231143, 2013.
- M. Coutelier, S. Andries, S. Ghariani, B. Dan, C. Duyckaerts, K. van Rijkevorsel, C. Raftopoulos, N. Deconinck, P. Sonderegger, F. Scaravilli, M. Vikkula, and C. Godfraind. Neuroserpin mutation causes electrical status epilepticus of slow-wave sleep. *Neurology*, 71(1):64–66, 2008.
- D. C. Crowther. Familial conformational diseases and dementias. *Hum Mutat*, 20(1):1–14, 2002.
- D. K. Dastur, B. S. Singhal, M. Gootz, and F. Seitelberger. Atypical inclusion bodies with myoclonic epilepsy. *Acta Neuropathologica*, 7(1):16–25, 1966.

- R. L. Davis, P. D. Holohan, A. E. Shrimpton, A. H. Tatum, J. Daucher, G. H. Collins, R. Todd, C. Bradshaw, P. Kent, D. Feiglin, A. Rosenbaum, M. S. Yerby, C.-M. Shaw, F. Lacbawan, and D. A. Lawrence. Familial Encephalopathy with Neuroserpin Inclusion Bodies. *The American Journal of Pathology*, 155(6):1901–1913, 1999a.
- R. L. Davis, A. E. Shrimpton, P. D. Holohan, C. Bradshaw, D. Feiglin, G. H. Collins, P. Sonderegger, J. Kinter, L. M. Becker, F. Lacbawan, D. Krasnewich, M. Muenke, D. A. Lawrence, M. S. Yerby, C.-M. Shaw, B. Gooptu, P. R. Elliott, J. T. Finch, R. W. Carrell, and D. A. Lomas. Familial dementia caused by polymerization of mutant neuroserpin. *Nature*, 401(6751):376–379, 1999b.
- R. L. Davis, A. E. Shrimpton, R. W. Carrell, D. A. Lomas, L. Gerhard, B. Baumann, D. A. Lawrence, M. Yepes, T. S. Kim, B. Ghetti, P. Piccardo, M. Takao, F. Lacbawan, M. Muenke, R. N. Sifers, C. B. Bradshaw, P. F. Kent, G. H. Collins, D. Larocca, and P. D. Holohan. Association between conformational mutations in neuroserpin and onset and severity of dementia. *Lancet*, 359(9325):2242–2247, 2002.
- C. L. Dolman. Atypical myoclonus body epilepsy (adult variant). *Acta Neuropathologica*, 31(3):201–206, 1975.
- P. R. Elliott, D. A. Lomas, R. W. Carrell, and J. P. Abrahams. Inhibitory conformation of the reactive loop of A1-antitrypsin. *Nature Structural & Molecular Biology*, 3(8):676–681, 1996.
- P. R. Elliott, X. Y. Pei, T. R. Dafforn, and D. A. Lomas. Topography of a 2.0 Å structure of A1-antitrypsin reveals targets for rational drug design to prevent conformational disease. *Protein Science*, 9(7):1274–1281, 2000.
- S. Fabbro and N. W. Seeds. Plasminogen activator activity is inhibited while neuroserpin is up-regulated in the Alzheimer disease brain. *J Neurochem*, 109(2):303–315, 2009.
- S. Fabbro, K. Schaller, and N. W. Seeds. Amyloid-beta levels are significantly reduced and spatial memory defects are rescued in a novel neuroserpin-deficient Alzheimer’s disease transgenic mouse model. *J Neurochem*, 118(5):928–938, 2011.
- M. Fernández-Monreal, J. P. López-Atalaya, K. Benchenane, M. Cacquevel, F. Dulin, J.-P. L. Caer, J. Rossier, A.-C. Jarrige, E. T. MacKenzie, N. Colloc’h, C. Ali, and D. Vivien. Arginine 260 of the Amino-terminal Domain of NR1 Subunit Is Critical for Tissue-type Plasminogen Activator-mediated Enhancement of

- N-Methyl-D-aspartate Receptor Signaling. *Journal of Biological Chemistry*, 279 (49):50850–50856, 2004.
- A. Fire, S. Xu, M. K. Montgomery, S. A. Kostas, S. E. Driver, and C. C. Mello. Potent and specific genetic interference by double-stranded RNA in *Caenorhabditis elegans*. *Nature*, 391(6669):806–811, 1998.
- L. Fredriksson, T. K. Stevenson, E. J. Su, M. Ragsdale, S. Moore, S. Craciun, G. P. Schielke, G. G. Murphy, and D. A. Lawrence. Identification of a neurovascular signaling pathway regulating seizures in mice. *Annals of Clinical and Translational Neurology*, 2(7):722–738, 2015.
- G. Galliciotti, M. Glatzel, J. Kinter, S. V. Kozlov, P. Cinelli, T. Rüllicke, and P. Sonderegger. Accumulation of Mutant Neuroserpin Precedes Development of Clinical Symptoms in Familial Encephalopathy with Neuroserpin Inclusion Bodies. *The American Journal of Pathology*, 170(4):1305–1313, 2007.
- M. Gelderblom, M. Neumann, P. Ludewig, C. Bernreuther, S. Krasemann, P. Arunachalam, C. Gerloff, M. Glatzel, and T. Magnus. Deficiency in serine protease inhibitor neuroserpin exacerbates ischemic brain injury by increased postischemic inflammation. *PLoS One*, 8(5):e63118, 2013.
- B. Gooptu and D. A. Lomas. Conformational Pathology of the Serpins: Themes, Variations, and Therapeutic Strategies. *Annual Review of Biochemistry*, 78(1):147–176, 2009.
- I. Gourfinkel-An, C. Duyckaerts, A. Camuzat, C. Meyrignac, P. Sonderegger, M. Baulac, and A. Brice. Clinical and neuropathologic study of a French family with a mutation in the neuroserpin gene. *Neurology*, 69(1):79–83, 2007.
- F. L. Graham, J. Smiley, W. C. Russell, and R. Nairn. Characteristics of a human cell line transformed by DNA from human adenovirus type 5. *The Journal of General Virology*, 36(1):59–74, 1977.
- R. P. Gu, L. L. Fu, C. H. Jiang, Y. F. Xu, X. Wang, and J. Yu. Retina Is Protected by Neuroserpin from Ischemic/Reperfusion-Induced Injury Independent of Tissue-Type Plasminogen Activator. *PLOS ONE*, 10(7):e0130440, 2015.
- N. A. Guadagno, C. Moriconi, V. Licursi, E. D’Acunto, P. S. Nisi, N. Carucci, A. De Jaco, E. Cacci, R. Negri, G. Lupo, and E. Miranda. Neuroserpin polymers cause oxidative stress in a neuronal model of the dementia FENIB. *Neurobiology of disease*, 103:32–44, 2017.

- S. Guo, S. L. Booten, M. Aghajan, G. Hung, C. Zhao, K. Blomenkamp, D. Gattis, A. Watt, S. M. Freier, J. H. Teckman, M. L. McCaleb, and B. P. Monia. Antisense oligonucleotide treatment ameliorates alpha-1 antitrypsin-related liver disease in mice. *The Journal of Clinical Investigation*, 124(1):251–261, 2014.
- M. C. Hagen, J. R. Murrell, M.-B. Delisle, E. Andermann, F. Andermann, M. C. Guiot, and B. Ghetti. Encephalopathy with Neuroserpin Inclusion Bodies Presenting as Progressive Myoclonus Epilepsy and Associated with a Novel Mutation in the Proteinase Inhibitor 12 Gene. *Brain Pathology*, 21(5):575–582, 2011.
- Y. Hakak, J. R. Walker, C. Li, W. H. Wong, K. L. Davis, J. D. Buxbaum, V. Haroutunian, and A. A. Fienberg. Genome-wide expression analysis reveals dysregulation of myelination-related genes in chronic schizophrenia. *Proceedings of the National Academy of Sciences*, 98(8):4746–4751, 2001.
- G. A. Hastings, T. A. Coleman, C. C. Haudenschild, S. Stefansson, E. P. Smith, R. Barthlow, S. Cherry, M. Sandkvist, and D. A. Lawrence. Neuroserpin, a brain-associated inhibitor of tissue plasminogen activator is localized primarily in neurons. Implications for the regulation of motor learning and neuronal survival. *Journal of Biological Chemistry*, 272(52):33062–33067, 1997.
- J. A. Huntington, R. J. Read, and R. W. Carrell. Structure of a serpin–protease complex shows inhibition by deformation. *Nature*, 407(6806):923–926, 2000.
- S. Ishigami, M. Sandkvist, F. Tsui, E. Moore, T. A. Coleman, and D. A. Lawrence. Identification of a novel targeting sequence for regulated secretion in the serine protease inhibitor neuroserpin. *Biochemical Journal*, 402(1):25–34, 2007.
- S. Kaushal, M. Annamali, K. Blomenkamp, D. Rudnick, D. Halloran, E. M. Brunt, and J. H. Teckman. Rapamycin reduces intrahepatic alpha-1-antitrypsin mutant Z protein polymers and liver injury in a mouse model. *Experimental Biology and Medicine (Maywood, N.J.)*, 235(6):700–709, 2010.
- K. J. Kinghorn, D. C. Crowther, L. K. Sharp, C. Nerelius, R. L. Davis, H. T. Chang, C. Green, D. C. Gubb, J. Johansson, and D. A. Lomas. Neuroserpin binds Abeta and is a neuroprotective component of amyloid plaques in Alzheimer disease. *J Biol Chem*, 281(39):29268–29277, 2006.
- A. C. Komor, Y. B. Kim, M. S. Packer, J. A. Zuris, and D. R. Liu. Programmable editing of a target base in genomic DNA without double-stranded DNA cleavage. *Nature*, 533(7603):420–424, 2016.

- H. Kroeger, E. Miranda, I. MacLeod, J. Perez, D. C. Crowther, S. J. Marciniak, and D. A. Lomas. ERAD and autophagy cooperate to degrade polymerogenic mutant serpins. *Journal of Biological Chemistry*, page jbc.M109.027102, 2009.
- S. R. Krueger, G. P. Ghisu, P. Cinelli, T. P. Gschwend, T. Osterwalder, D. P. Wolfer, and P. Sonderegger. Expression of neuroserpin, an inhibitor of tissue plasminogen activator, in the developing and adult nervous system of the mouse. *Journal of Neuroscience*, 17(23):8984–8996, 1997.
- N. Lebeurrier, G. Liot, J. P. Lopez-Atalaya, C. Orset, M. Fernandez-Monreal, P. Sonderegger, C. Ali, and D. Vivien. The brain-specific tissue-type plasminogen activator inhibitor, neuroserpin, protects neurons against excitotoxicity both in vitro and in vivo. *Mol Cell Neurosci*, 30(4):552–558, 2005.
- T. W. Lee, L. C. Coates, and N. P. Birch. Neuroserpin regulates N-cadherin-mediated cell adhesion independently of its activity as an inhibitor of tissue plasminogen activator. *Journal of Neuroscience Research*, 86(6):1243–1253, 2008.
- T. W. Lee, V. W. K. Tsang, and N. P. Birch. Physiological and pathological roles of tissue plasminogen activator and its inhibitor neuroserpin in the nervous system. *Frontiers in Cellular Neuroscience*, 9, 2015.
- T. W. Lee, V. W. K. Tsang, E. J. Loef, and N. P. Birch. Physiological and pathological functions of neuroserpin: Regulation of cellular responses through multiple mechanisms. *Seminars in Cell & Developmental Biology*, 62:152–159, 2017.
- Z. Lin, J. K. Jensen, Z. Hong, X. Shi, L. Hu, P. A. Andreasen, and M. Huang. Structural Insight into Inactivation of Plasminogen Activator Inhibitor-1 by a Small-Molecule Antagonist. *Chemistry & Biology*, 20(2):253–261, 2013.
- D. A. Lomas and R. W. Carrell. Serpinopathies and the conformational dementias. *Nat Rev Genet*, 3(10):759–768, 2002.
- D. A. Lomas, J. R. Hurst, and B. Gooptu. Update on alpha-1 antitrypsin deficiency: New therapies. *J Hepatol*, 65(2):413–424, 2016.
- R. Mahadeva, T. R. Dafforn, R. W. Carrell, and D. A. Lomas. 6-mer peptide selectively anneals to a pathogenic serpin conformation and blocks polymerization. Implications for the prevention of Z alpha(1)-antitrypsin-related cirrhosis. *Journal of Biological Chemistry*, 277(9):6771–6774, 2002.
- M. Mallya, R. L. Phillips, S. A. Saldanha, B. Gooptu, S. C. Leigh Brown, D. J. Termine, A. M. Shirvani, Y. Wu, R. N. Sifers, R. Abagyan, and D. A. Lomas.

- Small Molecules Block the Polymerization of Z A1-Antitrypsin and Increase the Clearance of Intracellular Aggregates. *Journal of Medicinal Chemistry*, 50(22): 5357–5363, 2007.
- E. Miranda, K. Römisch, and D. A. Lomas. Mutants of neuroserpin that cause dementia accumulate as polymers within the endoplasmic reticulum. *J Biol Chem*, 279(27):28283–28291, 2004.
- E. Miranda, I. MacLeod, M. J. Davies, J. Pérez, K. Römisch, D. C. Crowther, and D. A. Lomas. The intracellular accumulation of polymeric neuroserpin explains the severity of the dementia FENIB. *Hum Mol Genet*, 17(11):1527–1539, 2008.
- N. Motamedi-Shad, A. M. Jagger, M. Liedtke, S. V. Faull, A. S. Nanda, E. Salvadori, J. L. Wort, C. W. M. Kay, N. Heyer-Chauhan, E. Miranda, J. Perez, A. Ordóñez, I. Haq, J. A. Irving, and D. A. Lomas. An antibody that prevents serpin polymerisation acts by inducing a novel allosteric behaviour. *Biochemical Journal*, page BCJ20160159, 2016.
- C. Mueller and T. R. Flotte. Gene-Based Therapy for Alpha-1 Antitrypsin Deficiency. *COPD: Journal of Chronic Obstructive Pulmonary Disease*, 10(sup1): 44–49, 2013.
- O. Nicole, F. Docagne, C. Ali, I. Margaille, P. Carmeliet, E. T. MacKenzie, D. Vivien, and A. Buisson. The proteolytic activity of tissue-plasminogen activator enhances NMDA receptor-mediated signaling. *Nature Medicine*, 7(1):59–64, 2001.
- H. M. Nielsen, L. Minthon, E. Londos, K. Blennow, E. Miranda, J. Perez, D. C. Crowther, D. A. Lomas, and S. M. Janciauskiene. Plasma and CSF serpins in Alzheimer disease and dementia with Lewy bodies. *Neurology*, 69(16):1569–1579, 2007.
- F. Nitschke, S. J. Ahonen, S. Nitschke, S. Mitra, and B. A. Minassian. Lafora disease — from pathogenesis to treatment strategies. *Nature Reviews Neurology*, 14(10): 606, 2018.
- F. Oberhauser. *Beteiligung von OS-9 an Der ER-Assoziierten Degradation (ERAD) Bei Familiärer Enzephalopathie Mit Neuroserpin-Einschlüssen (FENIB)*. PhD thesis, University of Hamburg, 2013.
- A. Ordóñez, J. Pérez, L. Tan, J. A. Dickens, N. Motamedi-Shad, J. A. Irving, I. Haq, U. Ekeowa, S. J. Marciniak, E. Miranda, and D. A. Lomas. A single-chain variable fragment intrabody prevents intracellular polymerization of Z α_1

- antitrypsin while allowing its antiproteinase activity. *The FASEB Journal*, 29 (6):2667–2678, 2015.
- T. Osterwalder, J. Contartese, E. T. Stoeckli, T. B. Kuhn, and P. Sonderegger. Neuroserpin, an axonally secreted serine protease inhibitor. *EMBO Journal*, 15 (12):2944–2953, 1996.
- T. Osterwalder, P. Cinelli, A. Baici, A. Pennella, S. R. Krueger, S. P. Schrimpf, M. Meins, and P. Sonderegger. The axonally secreted serine proteinase inhibitor, neuroserpin, inhibits plasminogen activators and plasmin but not thrombin. *Journal of Biological Chemistry*, 273(4):2312–2321, 1998.
- T. Ota, Y. Hisatomi, K. Kashiwamura, K. Otsu, Y. Nakamura, S. Takamatsu, and P. Mehraein. Histochemistry and ultrastructure of atypical myoclonus body (type II). *Acta Neuropathologica*, 28(1):45–54, 1974.
- P. K. Parmar, L. C. Coates, J. F. Pearson, R. M. Hill, and N. P. Birch. Neuroserpin regulates neurite outgrowth in nerve growth factor-treated PC12 cells. *J Neurochem*, 82(6):1406–1415, 2002.
- R. J. Platt, S. Chen, Y. Zhou, M. J. Yim, L. Swiech, H. R. Kempton, J. E. Dahlman, O. Parnas, T. M. Eisenhaure, M. Jovanovic, D. B. Graham, S. Jhunjhunwala, M. Heidenreich, R. J. Xavier, R. Langer, D. G. Anderson, N. Hacohen, A. Regev, G. Feng, P. A. Sharp, and F. Zhang. CRISPR-Cas9 Knockin Mice for Genome Editing and Cancer Modeling. *Cell*, 159(2):440–455, 2014.
- M. Prince, M. Guerchet, and M. Prina. The global impact of dementia 2013-2050, 2013.
- Z. Qian, M. E. Gilbert, M. A. Colicos, E. R. Kandel, and D. Kuhl. Tissue-plasminogen activator is induced as an immediate-early gene during seizure, kindling and long-term potentiation. *Nature*, 361(6411):453–457, 1993.
- E. Ranza, S. Garcia-Tarodo, K. Varvagiannis, M. Guipponi, J. A. Lohrman, A. Bot-tani, I. Kern, M. Kurian, M.-P. Pittet, S. E. Antonarakis, J. Fluss, and C. M. Korff. SERPINI1 pathogenic variants: An emerging cause of childhood-onset progressive myoclonic epilepsy. *American Journal of Medical Genetics Part A*, 2017.
- R. Reumann, R. Vierk, L. Zhou, F. Gries, V. Kraus, J. Mienert, E. Romswinkel, F. Morellini, I. Ferrer, C. Nicolini, M. Fahnstock, G. Rune, M. Glatzel, and G. Galliciotti. The serine protease inhibitor neuroserpin is required for normal

- synaptic plasticity and regulates learning and social behavior. *Learning & Memory*, 24(12):650–659, 2017.
- R. Rodríguez-González, J. Agulla, M. Pérez-Mato, T. Sobrino, and J. Castillo. Neuroprotective effect of neuroserpin in rat primary cortical cultures after oxygen and glucose deprivation and tPA. *Neurochemistry International*, 58(3):337–343, 2011a.
- R. Rodríguez-González, M. Millán, T. Sobrino, E. Miranda, D. Brea, N. P. de la Ossa, M. Blanco, J. Perez, L. Dorado, M. Castellanos, D. A. Lomas, M. A. Moro, A. Dávalos, and J. Castillo. The natural tissue plasminogen activator inhibitor neuroserpin and acute ischaemic stroke outcome. *Thrombosis and Haemostasis*, 105(3):421–429, 2011b.
- B. D. Roussel, J. A. Irving, U. I. Ekeowa, D. Belorgey, I. Haq, A. Ordóñez, A. J. Kruppa, A. Duvoix, S. T. Rashid, D. C. Crowther, S. J. Marciniak, and D. A. Lomas. Unravelling the twists and turns of the serpinopathies. *The FEBS Journal*, pages 3859–3867, 2011.
- B. D. Roussel, T. M. Newton, E. Malzer, N. Simecek, I. Haq, S. E. Thomas, M. L. Burr, P. J. Lehner, D. C. Crowther, S. J. Marciniak, and D. A. Lomas. Sterol metabolism regulates neuroserpin polymer degradation in the absence of the unfolded protein response in the dementia FENIB. *Hum Mol Genet*, 22(22):4616–4626, 2013.
- S.-E. Ryu, H.-J. Choi, K.-S. Kwon, K. N. Lee, and M.-H. Yu. The native strains in the hydrophobic core and flexible reactive loop of a serine protease inhibitor: Crystal structure of an uncleaved A1-antitrypsin at 2.7 Å. *Structure*, 4(10):1181–1192, 1996.
- G. Saga, F. Sessa, A. Barbiroli, C. Santambrogio, R. Russo, M. Sala, S. Raccosta, V. Martorana, S. Caccia, R. Noto, C. Moriconi, E. Miranda, R. Grandori, M. Manno, M. Bolognesi, and S. Ricagno. Embelin binds to human neuroserpin and impairs its polymerisation. *Scientific Reports*, 6:18769, 2016.
- A. L. Samson, S. T. Nevin, D. Croucher, B. Niego, P. B. Daniel, T. W. Weiss, E. Moreno, D. Monard, D. A. Lawrence, and R. L. Medcalf. Tissue-type plasminogen activator requires a co-receptor to enhance NMDA receptor function. *Journal of Neurochemistry*, 107(4):1091–1101, 2008.
- J. Saraiva, R. J. Nobre, and L. Pereira de Almeida. Gene therapy for the CNS using AAVs: The impact of systemic delivery by AAV9. *Journal of Controlled Release*, 241:94–109, 2016.

- A. Schipanski, S. Lange, A. Segref, A. Gutschmidt, D. A. Lomas, E. Miranda, M. Schweizer, T. Hoppe, and M. Glatzel. A Novel Interaction Between Aging and ER Overload in a Protein Conformational Dementia. *Genetics*, 193(3):865–876, 2013.
- A. Schipanski, F. Oberhauser, M. Neumann, S. Lange, B. Szalay, S. Krasemann, F. W. van Leeuwen, G. Galliciotti, and M. Glatzel. The lectin OS-9 delivers mutant neuroserpin to endoplasmic reticulum associated degradation in familial encephalopathy with neuroserpin inclusion bodies. *Neurobiology of Aging*, 35(10):2394–2403, 2014.
- S. P. Schrimpf, A. J. Bleiker, L. Brecevic, S. V. Kozlov, P. Berger, T. Osterwalder, S. R. Krueger, A. Schinzel, and P. Sonderegger. Human neuroserpin (PI12): cDNA cloning and chromosomal localization to 3q26. *Genomics*, 40(1):55–62, 1997.
- D. J. Selkoe and J. Hardy. The amyloid hypothesis of Alzheimer’s disease at 25 years. *EMBO Molecular Medicine*, 8(6):595–608, 2016.
- G. A. Silverman, P. I. Bird, R. W. Carrell, F. C. Church, P. B. Coughlin, P. G. W. Gettins, J. A. Irving, D. A. Lomas, C. J. Luke, R. W. Moyer, P. A. Pemberton, E. Remold-O’Donnell, G. S. Salvesen, J. Travis, and J. C. Whisstock. The serpins are an expanding superfamily of structurally similar but functionally diverse proteins: evolution, mechanism of inhibition, novel functions, and a revised nomenclature. *Journal of Biological Chemistry*, 276(36):33293–33296, 2001.
- S. Sindi, F. Mangialasche, and M. Kivipelto. Advances in the prevention of Alzheimer’s Disease. *F1000Prime Reports*, 7, 2015.
- M. Takao, M. D. Benson, J. R. Murrell, M. Yazaki, P. Piccardo, F. W. Unverzagt, R. L. Davis, P. D. Holohan, D. A. Lawrence, R. Richardson, M. R. Farlow, and B. Ghetti. Neuroserpin mutation S52R causes neuroserpin accumulation in neurons and is associated with progressive myoclonus epilepsy. *J Neuropathol Exp Neurol*, 59(12):1070–1086, 2000.
- T. Teesalu, A. Kulla, A. Simisker, V. Sirén, D. A. Lawrence, T. Asser, and A. Vaheri. Tissue plasminogen activator and neuroserpin are widely expressed in the human central nervous system. *Thrombosis and Haemostasis*, 92(8):358–368, 2004.
- A. Tjärnlund-Wolf, S. Olsson, K. Jood, C. Blomstrand, and C. Jern. No evidence for an association between genetic variation at the SERPINI1 locus and ischemic stroke. *J Neurol*, 258(10):1885–1887, 2011.

- M. P. Vawter, T. Barrett, C. Cheadle, B. P. Sokolov, W. H. Wood, D. M. Donovan, M. Webster, W. J. Freed, and K. G. Becker. Application of cDNA microarrays to examine gene expression differences in schizophrenia. *Brain Research Bulletin*, 55(5):641–650, 2001.
- M. P. Vawter, C. Shannon Weickert, E. Ferran, M. Matsumoto, K. Overman, T. M. Hyde, D. R. Weinberger, W. E. Bunney, and J. E. Kleinman. Gene Expression of Metabolic Enzymes and a Protease Inhibitor in the Prefrontal Cortex Are Decreased in Schizophrenia. *Neurochem Res*, 29(6):1245–1255, 2004.
- H. T. Wright and J. N. Scarsdale. Structural basis for serpin inhibitor activity. *Proteins: Structure, Function, and Bioinformatics*, 22(3):210–225, 1995.
- S. Ye, A. L. Cech, R. Belmares, R. C. Bergstrom, Y. Tong, D. R. Corey, M. R. Kanost, and E. J. Goldsmith. The structure of a Michaelis serpin–protease complex. *Nature Structural & Molecular Biology*, 8(11):979–983, 2001.
- M. Yepes, M. Sandkvist, M. K. Wong, T. A. Coleman, E. Smith, S. L. Cohan, and D. A. Lawrence. Neuroserpin reduces cerebral infarct volume and protects neurons from ischemia-induced apoptosis. *Blood*, 96(2):569–576, 2000.
- M. Yepes, M. Sandkvist, T. A. Coleman, E. Moore, J.-Y. Wu, D. Mitola, T. H. Bugge, and D. A. Lawrence. Regulation of seizure spreading by neuroserpin and tissue-type plasminogen activator is plasminogen-independent. *J Clin Invest*, 109(12):1571–1578, 2002.
- M. Yepes, M. Sandkvist, E. G. Moore, T. H. Bugge, D. K. Strickland, and D. A. Lawrence. Tissue-type plasminogen activator induces opening of the blood-brain barrier via the LDL receptor–related protein. *The Journal of Clinical Investigation*, 112(10):1533–1540, 2003.
- M. S. Yerby, C. M. Shaw, and J. M. Watson. Progressive dementia and epilepsy in a young adult: Unusual intraneuronal inclusions. *Neurology*, 36(1):68–71, 1986.
- Z. Ying, H. Wang, H. Fan, and G. Wang. The endoplasmic reticulum (ER)-associated degradation system regulates aggregation and degradation of mutant neuroserpin. *J Biol Chem*, 286(23):20835–20844, 2011.
- K. Yusa, S. T. Rashid, H. Strick-Marchand, I. Varela, P.-Q. Liu, D. E. Paschon, E. Miranda, A. Ordóñez, N. R. F. Hannan, F. J. Rouhani, S. Darche, G. Alexander, S. J. Marciniak, N. Fusaki, M. Hasegawa, M. C. Holmes, J. P. Di Santo, D. A. Lomas, A. Bradley, and L. Vallier. Targeted gene correction of A_1 -antitrypsin deficiency in induced pluripotent stem cells. *Nature*, 478(7369):391–394, 2011.

Z. Zhang, L. Zhang, M. Yepes, Q. Jiang, Q. Li, P. Arniago, T. A. Coleman, D. A. Lawrence, and M. Chopp. Adjuvant treatment with neuroserpin increases the therapeutic window for tissue-type plasminogen activator administration in a rat model of embolic stroke. *Circulation*, 106(6):740–745, 2002.

Acknowledgements

The preparation of this dissertation was an interesting and life changing journey. Along its way, there were many educational, rewarding and even funny and joyful moments while working in the lab or preparing the manuscript in the library. Certainly, however, the spectrum of emotions also included some tedious and frustrating times as befits a scholarly work.

Whereas nobody but fate and coincidence are to blame for the latter, I would very much like to thank all the people involved in the former. Learning from and together with you made me realize that this is something I would like to do for the rest of my life: Learning from and together with amazing people.

I would like to especially thank my two mentors in this project: Markus Glatzel (my Doktorvater) and Giovanna Galliciotti (my supervisor and basically my Doktormutter).

Markus kindly introduced me to the GRK 1459. This scholarship made it possible for me to pause my medical studies and focus on the experiments in full time. Furthermore, the weekly progress seminars and journal clubs at the Department of Neuropathology that Markus accommodated, provided for a friendly and helpful research environment. The thoughtful advice given at these meetings by Markus and others were gratefully included in this work.

Undoubtedly the biggest impact on the completion of this manuscript is owing to Giovanna. For every step — from the first experiment in the laboratory to the reviewing of the last paragraph — Giovanna took a tremendous amount of time and patience to teach me everything from basic biochemical methods to sophisticated scientific writing. Every mentee can only hope for such an amazing mentor.

Last but not least, I would like to thank my parents, Dagmar and Friedrich Ingwersen. Without their constant and unconditional support, inspiration and encouragement I would not be where I am today.

Lebenslauf wurde aus datentechnischen Gründen entfernt.

Eidesstattliche Versicherung

Ich versichere ausdrücklich, dass ich die Arbeit selbständig und ohne fremde Hilfe verfasst, andere als die von mir angegebenen Quellen und Hilfsmittel nicht benutzt und die aus den benutzten Werken wörtlich oder inhaltlich entnommenen Stellen einzeln nach Ausgabe (Auflage und Jahr des Erscheinens), Band und Seite des benutzten Werkes kenntlich gemacht habe.

Ferner versichere ich, dass ich die Dissertation bisher nicht einem Fachvertreter an einer anderen Hochschule zur Überprüfung vorgelegt oder mich anderweitig um Zulassung zur Promotion beworben habe.

Ich erkläre mich einverstanden, dass meine Dissertation vom Dekanat der Medizinischen Fakultät mit einer gängigen Software zur Erkennung von Plagiaten überprüft werden kann.

Unterschrift: